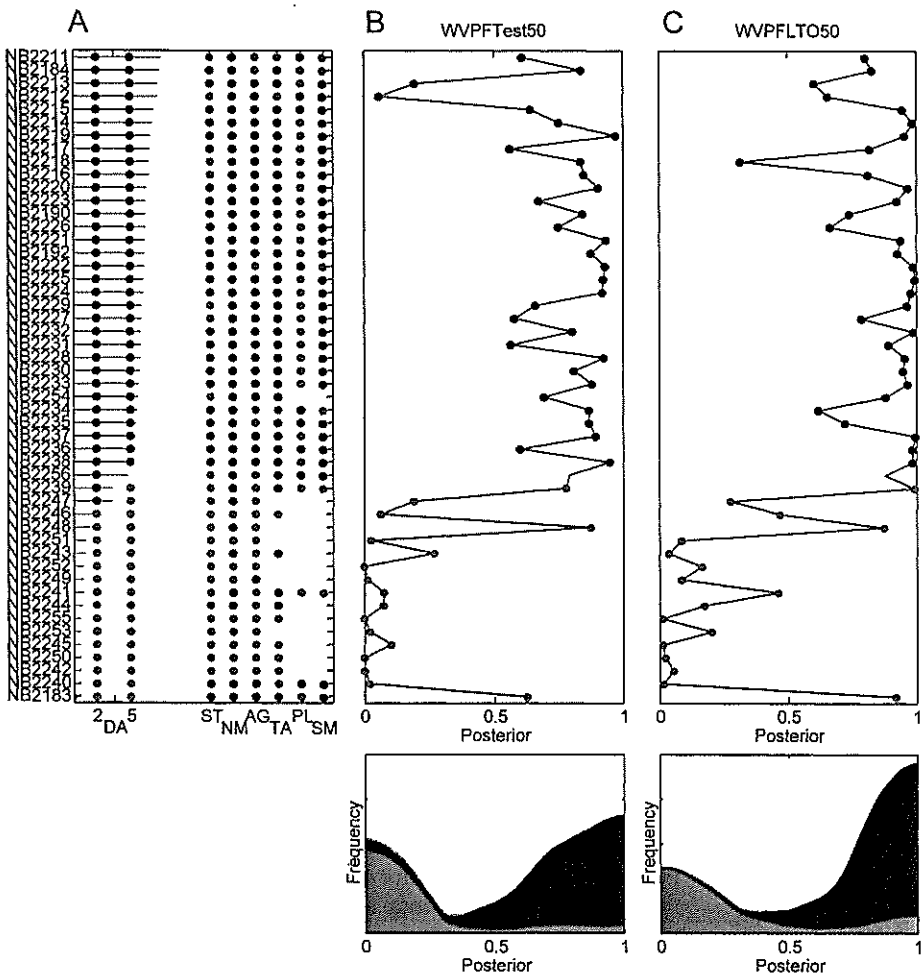

Figure 4. Posterior probability of survival at 5 years for test samples

Posterior probability of survival at 5 years for 50 independent test samples measured by newly developed 200 genes chip (the mini-chip system). Left panel: Neuroblastoma samples; see also Figure 2 legend. Center panel: Prediction results when the supervised classifier constructed from 96 training samples is applied to the 50 independent samples (independent test for the classifier's reproducibility). Right panel: LTO crossvalidation analysis using the new 50 samples (test for the procedure's reproducibility). Both tests do not introduce any information leakage. Lower panels: Smooth histograms of posterior probabilities for dead (red) and alive (blue) patients.

three things. (1) The supervised classifier obtained by the statistical analysis by the 5340 genes system is reproducible even if it is applied to the data measured by the reduced 200 genes system. Note that the 50 samples were completely new data for the classifier in this case. (2) Our procedure to construct a supervised classifier according to the LTO analysis is also reproducible, because the same procedure was successful in making another classifier with a high prediction accuracy when applied to the data taken by the mini-chip system. (3) A simple, low-cost microarray system, the mini-chip system, is highly feasible for predicting the prognosis of neuroblastoma.

Genes selected for prognosis prediction

To assess the relationship between the clinically defined subsets of neuroblastoma and the expression of 70 genes that were selected as top scored with 2 year prognosis according to the pairwise *F* score, we conducted an unsupervised clustering analysis (Figure 5). As expected, part of the type II (intermediate) tumors of patients with a poor prognosis showed an expression pattern that was similar to that of the type III (unfavorable) tumors, and many of them died. On the other hand, expression profiles of the remaining type II tumors seemed to be heterogeneous similarly to those of the type I (favorable) tumors with a good outcome. Most of the tumors with highly expressed *TrkA* and hyperdiploidy, as well as tumors detected by mass screening, were included in the latter group. Table 2 shows a list of 41 genes that corresponded to the 70 top-scored genes and their p and q values (Storey and Tibshirani, 2003) in the log rank test, since we found that several genes were duplicated in the selected 70 genes. Based on the above clustering, these genes were categorized into two groups (group F and group UF; the gene groups strongly correlated with favorable and unfavorable prognosis, respectively) (Figure 5 and Table 2).

The genes in group F tended to show high levels of expression in the type I tumors, while those in group UF were highly expressed in the type III tumors. The former contained genes that were related to neuronal differentiation (*tubulin* α, *peripherin*, *neuromodulin* [*GAP43*], and *HMP19*) and genes that were related to catecholamine metabolism (*dopa decarboxylase* [*DDC*], *dopamine* β-*hydroxylase* [*DBH*], and *tyrosine hydroxylase* [*TH*]). On the other hand, the latter involved many members of genes that are related to protein synthesis (ribosomal protein genes such as *RPL18A*, *RPLP0*, *RPL5*, *RPL4*, and *RPL7A* as well as translation initiation and elongation factor genes *EEF1G* and *EIF3S5*) and genes that are related to me-

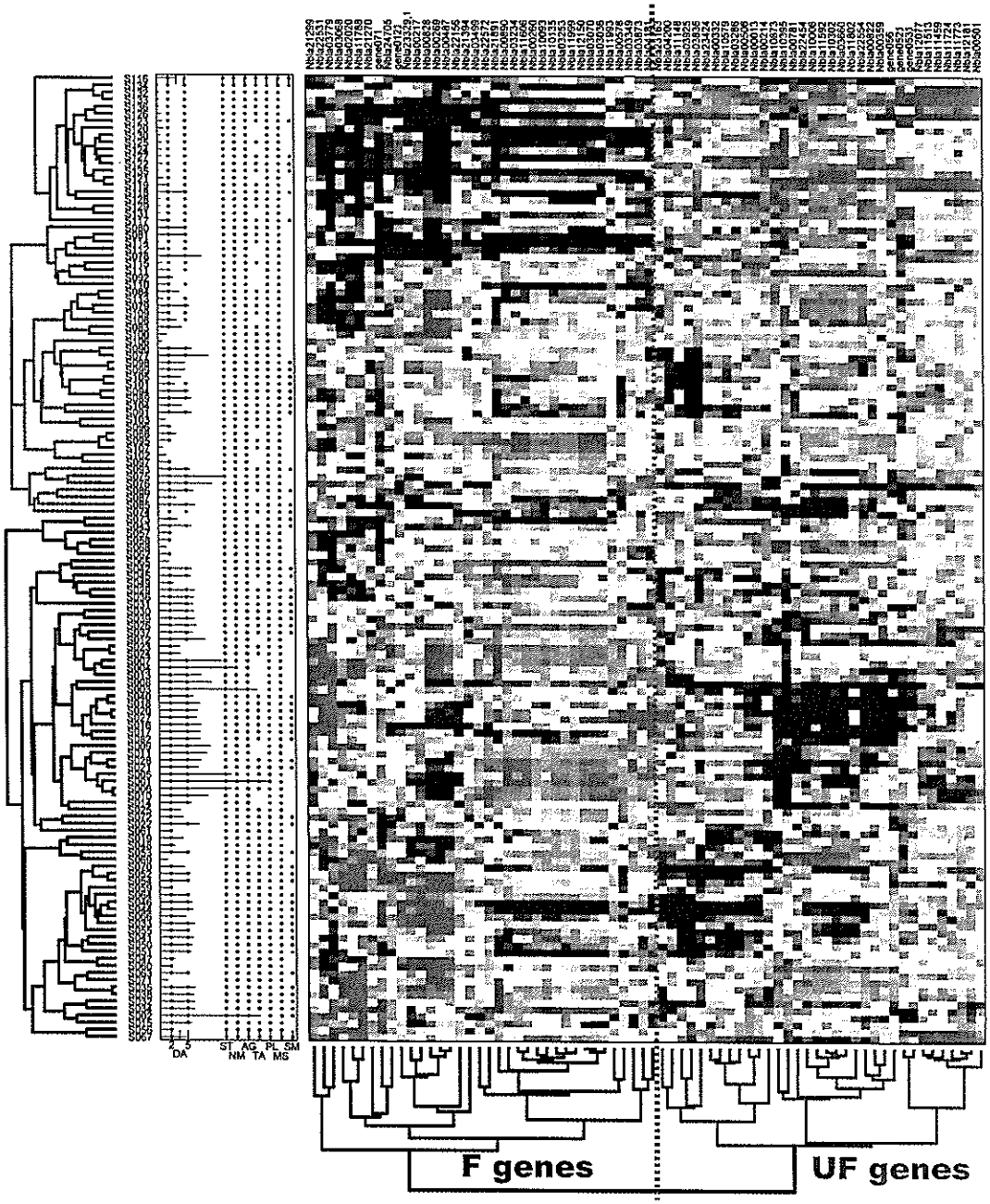

Figure 5. Expression profiles of 70 genes selected for predicting neuroblastoma prognosis at 2 years

Note that 10 genes for predicting prognosis at 5 years are also included in the 70 genes. The left and lower trees depict hierarchical clustering of the 136 neuroblastoma samples and the 70 genes selected in the present study, respectively. In the left tree, blue, green, and red colors denote "*MYCN* single and stage 1, 2 or 4s tumor" (type I, favorable), "*MYCN* single and stage 3, 4 tumor" (type II, intermediate), and "*MYCN* amplified tumor" (type III, unfavorable), respectively. The blue and red colors in the expression matrix show the high and low expression, respectively. A gene showing high expression level likely for unfavorable samples belongs to the group "UF" (red subtree in the lower tree), while one showing high expression likely for favorable samples belongs to the group "F" (blue subtree in the lower tree).

tabolism (*enolase 1* [*ENO1*] and *transketolase* [*TKT*]). The top 10 genes selected for the 5 year outcome prediction were *RPL18A*, *ENO1*, *EEF1G*, *TUBA3*, *GNB2L1*, *ARHGEF7*, *GCC2*, *DDX1* (duplicated), and *PRPH*. The *MYCN* gene was also a member of 70 genes (group UF) as expected; however, it was outside of the top 10 genes for the 5 year label. Instead, *DDX1*, which is frequently coamplified with *MYCN* on chromosome 2p24, was a member of the top 10 genes (UF group) for both of the 2 year and 5 year labels. Confirmation of the differential expression of the selected genes was further conducted by

Table 2. Top-ranked genes used for prediction of 2 year and 5 year prognosis of neuroblastoma

	Spot name	Accession number	Gene code	Chromosome map	Pattern	Log rank p	q value
F group							
	Nbla11606	NM_006009	*TUBA3*	12q13.12	F > UF	0	0.000674
	Nbla00890	NM_003899	*ARHGEF7*	13q34	F > UF	0.000001	0.000743
	Nbla00260	NM_006082	*K-ALPHA-1*	12q13.12	F > UF	0.000003	0.000926
	Nbla21891	U87309	*VPS41*	7p14.1	F > UF	0.000006	0.001096
	Nbla03873	NM_006054	*RTN3*	11q13.1	F > UF	0.00001	0.001282
	Nbla11788	NM_006262	*PRPH*	12q13.12	F > UF	0.000017	0.001522
	Nbla10093	NM_000183	*HADHB*	2p23.3	F > UF	0.000018	0.001541
	Nbla22572	NM_000790	*DDC*	7p12.2	F > UF	0.000035	0.00213
	Nbla21270	NM_001915	*CYB561*	17q23.3	F > UF	0.00016	0.00495
	gene071	NM_000360	*TH*	11p15.5	F > UF	0.000787	0.012173
	Nbla03499	NM_002074	*GNB1*	1p36.33	F > UF	0.000795	0.012237
	Nbla04181	AK55112	*AK55112*	5q13.2	F > UF	0.001425	0.017462
	Nbla00487	AB075512	*C6orf134*	6p21.33	F > UF	0.002751	0.025273
	Nbla00269	NM_000787	*DBH*	9q34.2	F > UF	0.00362	0.030407
	Nbla22531	NM_002045	*GAP43*	3q13.31	F > UF	0.004394	0.034175
	Nbla22156	NM_014944	*CLSTN1*	1p36.22	F > UF	0.005233	0.038274
	Nbla00578	NM_006818	*AF1Q*	1q21.3	F > UF	0.009397	0.05354
	Nbla00217	NM_032638	*GATA2*	3q21.3	F > UF	0.010245	0.056301
	Nbla21394	NM_000743	*CHRNA3*	15q25.1	F > UF	0.072464	0.162629
	Nbla11993	NM_015980	*HMP19*	5q35.2	F > UF	0.204274	0.282486
UF group							
	Nbla00214	NM_000980	*RPL18A*	19p13.11	F < UF	0.000002	0.001107
	Nbla00013	NM_006098	*GNB2L1*	5q35.3	F < UF	0.000006	0.001051
	Nbla11459	NM_004939	*DDX1*	2p24.3	F < UF	0.000024	0.001795
	Nbla11148	NM_001002	*RPLP0*	12q24.23	F < UF	0.000049	0.002549
	Nbla00332	NM_001404	*EEF1G*	11q12.3	F < UF	0.000055	0.002696
	Nbla10395	NM_002593	*PCOLCE*	7q22.1	F < UF	0.000164	0.005009
	Nbla03286	NM_020198	*GK001*	17q23.3	F < UF	0.000175	0.005204
	Nbla23163	NM_003754	*EIF3S5*	11p15.4	F < UF	0.000341	0.007105
	Nbla10579	NM_181453	*GCC2*	2q12.3	F < UF	0.000962	0.01407
	Nbla00359	NM_003550	*MAD1L1*	7p22.3	F < UF	0.00112	0.01525
	gene052-1	NM_005378	*MYCN*	2p24.3	F < UF	0.001253	0.016367
	Nbla03925	NM_002295	*LAMR1*	3p22.2	F < UF	0.001773	0.01931
	Nbla23424	NM_001404	*EEF1G*	11q12.3	F < UF	0.003579	0.030326
	Nbla22554	NM_000687	*AHCY*	20q11.22	F < UF	0.003946	0.032409
	gene056	NM_000546	*TP53*	17p13.1	F < UF	0.004087	0.032829
	Nbla10873	NM_005762	*TRIM28*	19q13.43	F < UF	0.004984	0.037476
	Nbla00501	NM_000969	*RPL5*	1p22.1	F < UF	0.005786	0.04012
	Nbla10302	NM_001428	*ENO1*	1p36.23	F < UF	0.007702	0.048179
	Nbla04200	NM_000968	*RPL4*	15q22.31	F < UF	0.04097	0.120453
	Nbla03836	NM_000972	*RPL7A*	9q34.2	F < UF	0.048031	0.132345
	Nbla00781	NM_001064	*TKT*	3p21.1	F < UF	0.048075	0.132342

Although 70 clones were selected as important genes for the supervised classifier, duplicated and multiplicated clones are omitted in this table. The 41 genes are classified into two groups, "F > UF" and "F < UF," when the expression in favorable samples is higher than that in unfavorable samples, and vice versa, respectively. In each group, genes are sorted by log rank p values. The log rank p value for each gene was calculated by comparing survival curves of two patient groups, in which the expression of the gene is higher and lower, respectively, than the median over the samples. A "q value" of a gene denotes the estimated false discovery rate among the genes whose p value is the same or smaller than that of the gene, and is a p-like value while incorporating multiplicity of the statistical test.

using representative 16 favorable and 16 unfavorable tumor samples that were independent of the 136 samples used in the present analysis, by semiquantitative RT-PCR (Figure S6; refer also to Ohira et al., 2003a). We also conducted immunohistochemical analysis for peripherin antibody using tissue sections prepared from primary neuroblastoma with favorable and unfavorable histology, since peripherin gene is a member of the top 10 genes for both 2 year and 5 year outcome prediction (Table 2). Peripherin protein was positively detected in the cytoplasm of neuroblastic cells as well as neuritis in all three favorable histology tumors (Figure S7, FH&NA). Two unfavorable histology tumors with poorly differentiated subtype, regardless of *MYCN* status, showed sporadic staining (less than 20% of the favorable histology tumor) for peripherin protein in neurites. Peripherin was completely negative in the unfavorable histology tumor of undifferentiated subtype (Figure S7, UF&NA). These results indicate the reliability of our gene selection. In the log rank test, p values of 18 of 20 genes in group F and of all 21 genes in group UF were less than 0.05 (Table 2), indicating that these 39 genes can be independent prognostic factors for primary neuroblastomas.

Discussion

Our study has disclosed the molecular signature of neuroblastoma that predicts patient outcomes by using RNA ob-

tained from 136 primary neuroblastomas. The highly reliable statistical analysis by using a neuroblastoma proper cDNA microarray harboring 5340 genes based on an electrically controlled ceramics-based ink-jet method led us to design a cDNA microarray system harboring 200 genes, which is applicable to short-term (2 year) and long-term (5 year) prognosis predictions for neuroblastoma.

Our study demonstrated that the supervised classifier produced by the 5340 genes system provided a high accuracy (88.5%) for the 5 year outcome prediction, with a good balance between sensitivity (86.7%) and specificity (89.4%). Although age at diagnosis, disease stage, *MYCN* amplification, and patients found by mass screening have been useful prognostic markers currently used at the bedside, most of them have either high sensitivity or high specificity (Table 1). The microarray analysis showed the best sensitivity-specificity balance among the prognostic factors for predicting the outcome of neuroblastoma. When the classifier is combined with the age at diagnosis, the disease stage (stage 1, 2, or 4s versus stage 3 or 4) and the *MYCN* amplification, accuracy, sensitivity, and specificity increased up to 95.8%, 93.3%, and 97.0%, respectively. Furthermore, the intermediate subset of neuroblastomas (type II), for which a long-term prognosis is usually difficult to make, was also categorized by microarray analysis into groups of patients with a favorable prognosis and those with an unfavorable prognosis. These successful results led us to produce a more practical tool at the bedside, the mini-chip system, whose accuracy, sensitivity, and specificity were 87.8%, 76.5%, and 93.8%, respectively, when the classifier constructed by the 5340 genes system was applied to 50 independent samples measured by the mini-chip system, and were 91.8%, 82.4% and 96.9%, respectively, when another classifier was constructed by applying the LTO procedure to the same data (Figure 4).

It is well recognized now that gene expression analyses for cancer prognosis prediction should pay close attention to the reproducibility of obtained results. A complete crossvalidation analysis without introducing any information leakage and an independent test using new samples are necessary. Although the determination of the appropriate number of genes used in supervised classifiers should be included in the validation procedure, it has often been ignored in most microarray studies. van 't Veer et al. (2002) applied the supervised classification to the breast cancer gene signature, which is predictive of a short interval to distant metastases in 78 patients who were initially devoid of local lymph node metastasis. Although their crossvalidation analysis without the validation of the number of genes correctly predicted the actual outcome of disease for 63 of 78 patients (80.7%), the accuracy was worse when a complete validation was applied (73.1%). This difference suggests that even small information leakage may lead to overestimation of the accuracy. Beer et al. (2002) applied the supervised classification to the outcome prediction of lung adenocarcinoma. Their statistical analysis was complete without any information leakage. They did not report the prediction accuracy, but we estimated the accuracy to be about 70% from the data in their paper and found that the prediction by their supervised classifier was not very superior to that by existing prognosis markers. Iizuka et al. (2003) applied the supervised classification to the prediction of intrahepatic recurrence within 1 year after curative surgery for hepatocellular carcinoma patients. Although their predictor showed sufficiently high accuracy in an independent test with 27 samples, their crossvalidation procedure excluded the validation of the determination process of the number of optimum genes (steps 5 and 6 in their algorithm). The high crossvalidation accuracy of 100% may be an overestimation due to the information leakage.

According to the recent study that evaluated statistical methodologies used by microarray studies published between 1995 and April 2003, the three papers above were the only ones that reported both fairly sound crossvalidation analyses and independent tests (Ntzani and Ioannidis, 2003). Our LTO procedure includes the validation process of the number of genes used in the classifier and hence is a complete crossvalidation process. In addition, the obtained classifier was applied to the 50 independent samples that were measured by the reduced 200 genes system. This is a stronger test than usual independent tests but is important for the development of a practical system at the bedside. In addition, our LTO analysis achieved an almost unbiased estimation of the accuracy. Our crossvalidation analysis using the LTO procedure, the independent test of the classifier, and the validation of the procedure itself within a new experimental environment using the mini-chip system exhibited one of the most conservative and reliable statistical methodologies. In addition, our gene selection procedure according to the pairwise F score tries to extract correlation structures among genes, based on an idea similar to the exhaustive optimization method used in Iizuka et al. (2003), is beneficial in enhancing the applicability of the mini-chip system to various prediction problems, namely, short-term and long-term outcome predictions.

In addition to high accuracy, another advantage of our method is to provide a type of predictive information beyond the conventional binary prediction like favorable and unfavorable, which is ambiguous. The probabilistic output based on the hypothetical distribution obtained by the LTO analysis, the posterior probability, was found to show good accordance with actual survival rate (right bottom panel in Figure 2); this enables us to make a simple interpretation of the output: a patient with a posterior value of 0.8 has 80% chance for the 5 year survival, for example. Moreover, by calculating posterior probabilities for various future time points, a survival chance curve for each patient can be depicted (Figure 6). Although the follow-up period of patient "S057" is 2 years, and the patient is alive at this time, the individual survival chance curve says that his/her survival chance estimated from the gene expression pattern at diagnosis will get smaller than 50% at about 3 years after diagnosis. Such an individual survival chance curve can be used in choosing a suitable therapeutic protocol.

Another advantage of our method is that the probabilistic output is very stable in the presence of noise. Even when an artificial noise, whose variance is as large as the estimated noise variance of microarray, was added to expression profile data, prognosis prediction did not degrade very much (Figure S8). This robustness was confirmed when the noise variance went up to 1.0, which was sufficiently greater than the actual reproduction noise level of 0.4 (Figures S1A–S1C).

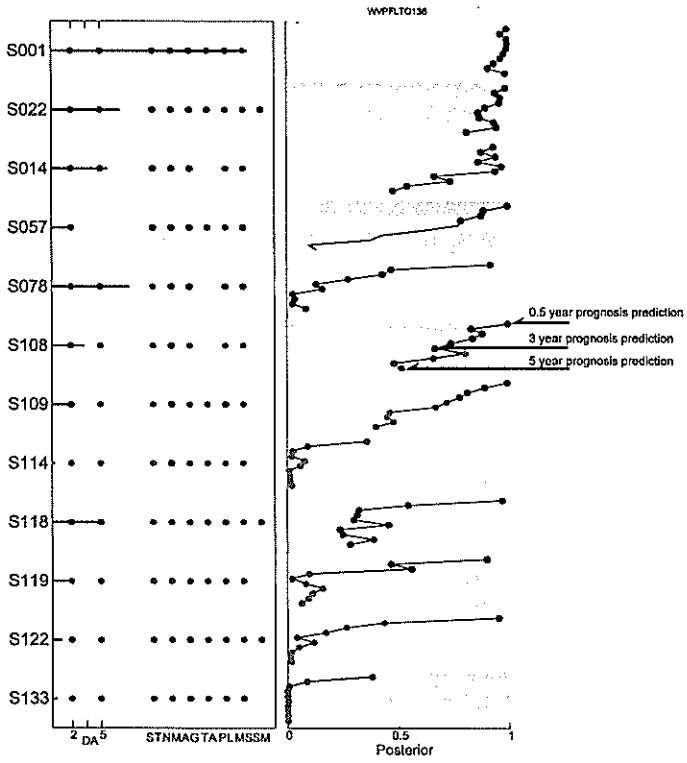

Figure 6. Individual survival chance analysis based on posterior probabilities

LTO estimation of survival probabilities at 0.5, 1.0, 1.5, ..., 5.0 years after diagnosis for 12 typical patients. Left panel: Information of patients (see caption of Figure 2). Right panel: Estimated posterior probabilities at 0.5, 1.0, 1.5, ..., 5.0 years after diagnosis, which predict the time course of patient's survival chance. A blue or a red mark denotes that the patient is alive or dead at that time after diagnosis, respectively. For example, the patient "S108," who died at 40 months, is predicted as 100% alive at 0.5 year and 52% alive at 5 year, solely from the microarray analysis at the diagnosis

The high outcome predictability of our system is attributable to multiple reasons. The quality of tumor samples is high because (1) an appropriate system was established for our neuroblastoma tissue bank, and (2) handling of tumor tissues is rather uniform at each hospital, in which informed consent was obtained. An array, produced by a new apparatus equipped with a piezo microceramic pump, generates highly reproducible signals. The noncontact spotting method makes the spot shape almost a perfect circle. Consequently, the spot excels in signal uniformity. We did not conduct microdissection of the 136 tumor samples, because the stromal components of the tumor, e.g., Schwannian cells, are already known to be very important to characterize its biology (Ambros and Ambros, 1995; Ambros and Ambros, 2000). Therefore, a good combination or selection of these procedures may have provided high outcome predictability. In addition, the high predictability was reliably confirmed by the complete crossvalidation analysis and the independent test. The probabilistic output based on the LTO analysis can provide a new type of information that will improve the therapeutic decision at the bedside. In addition, the probabilistic output is highly robust against noises that may be involved in test samples (described above); this can be the major reason for the high prediction accuracy when the classifier constructed by the 5340 genes system was applied to the data taken by the mini-chip system.

The impact of the selected genes is strong. The genes with the highest score in F group genes (F > UF) were *tubulin* α members (*TUBA3* and *K-ALPHA-1*, which corresponds to *TUBA1*), which have never been reported to be prognostic factors in neuroblastoma. Their prognostic significance has also been confirmed by RT-PCR in primary tumors (data not shown). The high expression of *TUBA1* in neuronal cells is associated with axonal outgrowth during development as well as with axonal degeneration after axotomy in adult animals (Knoops and Octave, 1997). The expression of *TUBA3* has been reported to be restricted to adherent, morphologically differentiated neuronal and glial cells (Hall and Cowan, 1985). We have also found that high expression of *tubulin tyrosine ligase* and enhanced tubulin tyrosination/detyrosination cycle are associated with neuronal differentiation in neuroblastomas with favorable prognosis (Kato et al., 2004). Thus, high mRNA expression of *TUBA* genes in favorable neuroblastoma may reflect differentiated status of tumors. ARHGEF7, Rho guanine nucleotide exchange factor 7, activates Rho proteins by exchanging bound GDP for GTP and can induce membrane ruffling. In our previous paper, we found that many family members of such G protein-related genes are highly expressed in favorable neuroblastomas compared to unfavorable ones (Ohira et al., 2003a). This may also imply a neuronal maturity nature of favorable tumors. Peripherin, a type III intermediate filament protein, was initially found as a cytoskeletal protein in the peripheral nervous system and in cultured cells of neuronal origin. This protein is known to be a marker of terminal neuronal differentiation; however, its functional role in neuroblastoma has been elusive. The previous evidence indicates that peripherin is transcriptionally upregulated by treatment with NGF, an important neurotrophin in neuroblastoma, and that the protein product is directly phosphorylated by NGF receptor, TrkA (Aletta et al., 1989). Thus, peripherin may play an important role as one of the signal transduction components involved in elaboration and maintenance of neuronal differentiation. In the UF gene group, many ribosomal protein-related genes are selected. *GNB2L1*, a receptor for activated C-kinase *RACK1*, is implicated in linking between *PKC* signaling and ribosome activation (Ceci et al., 2003). The *DDX1* gene, which is frequently coamplified with the *MYCN* gene in advanced neuroblastomas (Godbout and Squire, 1993; Noguchi et al., 1996), is also a member of this group. Its protein product is a putative RNA helicase and is implicated in a number of cellular processes involving alteration of RNA secondary structure such as translation initiation, nuclear and mitochondrial splicing, and ribosome and spliceosome assembly. *DDX1* is ranked at a higher score than the *MYCN* gene, which is concordant with the previous reports describing that *MYCN* mRNA expression is a weaker prognostic marker than its genomic amplification (Slavc et al., 1990). Another important prognostic factor, *TrkA*, is not included in the top 70 genes but in the 90 (in the top 20 genes when the 5 year label was used) (data not shown), probably due to its relatively low levels of mRNA expression as compared with those of other genes. The prognos-

tic effect of *TrkA* expression may be compensated by other genes which are affected or regulated by *TrkA* intracellular signaling. Similarly, *MYCN*-regulated genes such as ribosomal genes, translation initiation and elongation factors, and laminin receptor may compensate the effect of *MYCN* gene expression in aggressive tumors. It is intriguing that high mRNA expression of *p53* gene is also strongly related to unfavorable outcome. Although *p53* mutation is rare in primary neuroblastomas, and its gene product frequently accumulated in cytoplasm, an unknown mechanism that upregulates *p53* expression in aggressive tumors may exist.

Our results showed that the decision by majority by the genes selected based on microarray data alone can be a prognostic indicator comparative to the existing prognostic markers, and that the addition of the microarray data to the prognosis markers improved the outcome prediction (Table 1). The outcomes of patients belonging to the intermediate subset, whose prognosis prediction had been very difficult by existing prognosis markers, were effectively separated into favorable group and unfavorable group ($p < 10^{-4}$). The posterior value will help the decision of therapeutic modalities, and outcome prediction based on the posterior value is extremely robust against a possible noise. In addition, our practical, low-cost microarray carrying only 200 genes should make its clinical use possible. Our further validation by hybridizing RNA obtained from 50 fresh neuroblastomas on the 200 cDNAs microarray in a completely independent laboratory indicated that our prediction system is consistent and feasible. Therefore, the application of a highly qualified cDNA microarray at the bedside may bring tailored medicine that allows better treatment of neuroblastoma patients.

Experimental procedures

Patients and tumor specimens

Fresh, frozen tumor tissues were sent to the Division of Biochemistry, Chiba Cancer Center Research Institute, from a number of hospitals in Japan (1996–2002). Informed consent was obtained at each institution or hospital. We randomly selected tumor samples from this neuroblastoma tissue bank and then successfully conducted hybridization in 136 neuroblastomas consisting of 41 stage 1 tumors, 22 stage 2 tumors, 33 stage 3 tumors, 28 stage 4 tumors, and 12 stage 4s tumors. Among the 136 fresh neuroblastomas, seventeen tumors were obtained at the delayed primary surgery after giving chemotherapy, but the other 119 tumors were resected by biopsy or surgery without giving any therapy. After surgery, patients were treated according to the previously described common protocols (Kaneko et al., 1998). Biological information on each tumor, including *MYCN* gene copy number, *TrkA* gene expression, and DNA ploidy, was analyzed in our laboratory, as described previously (Hishiki et al., 1998). All the tumors were classified according to the International Neuroblastoma Staging System (INSS) (Brodeur et al., 1993). The stage 4s neuroblastoma shows a special pattern of clinical behaviors, and the tumor itself, as well as its widespread metastases to the skin, liver, or bone marrow, usually regresses spontaneously. For a better understanding of statistical results, we introduced Brodeur's classification of neuroblastoma subsets: type I (stages 1, 2, or 4s; a single copy of *MYCN*; blue marks in Figure 2), type II (stage 3 or 4; a single copy of *MYCN*; green marks in Figure 2), and type III (all stages; amplification of *MYCN*; red marks in Figure 2) (Brodeur and Nakagawara, 1992). Among 136 tumors that we analyzed, 66 were found by mass screening of urinary catecholamine metabolites at the age of 6 months, which has been performed nationwide in Japan from 1984 to 2004 (Sawada et al., 1984). The follow-up duration ranged between 3 and 241 months (median, 56 months; mean, 57.3 months) after diagnosis. All diagnoses of neuroblastoma were confirmed by the histological assessment of a surgically resected tumor specimen at each hospital. Shimada's classification (Shimada et al., 1984) was performed in 62 out of 136 cases. The macroscopic necroses in the tumor were excluded from the tissue sampling for molecular analysis. We used for the microarray analysis only the tumor samples whose adjacent tissues contained more than 70% tumor cells in the thin sections stained with hematoxylin-eosin. For independent test, 50 (19 were found by mass screening and 31 were clinically found) tumors (15 of stage 1, 6 of stage 2, 9 of stage 3, 14 of stage 4, and 6 of stage 4s) were used.

Total RNA was extracted from each frozen tissue according to the AGPC method (Chomczynski and Sacchi, 1987). RNA integrity, quality, and quantity were then assessed by electrophoresis on the Agilent RNA 6000 nanochip using Agilent 2100 BioAnalyzer (Agilent Technologies, Inc.).

cDNA microarray experiments

We previously obtained approximately 5,000 genes after selecting from 10,000 clones randomly picked up from the mixture of oligo-capping cDNA libraries, which were generated from three primary neuroblastomas with a favorable outcome (stage 1; high *TrkA* expression and a single copy of *MYCN*), three tumors with a poor prognosis (stage 3 or 4; low expression of *TrkA* and amplification of *MYCN*), and a stage 4s tumor (Ohira et al., 2003a; Ohira et al., 2003b). Using these isolated genes together with 80 known cDNAs that were thought to be neuroblastoma-related genes, we first constructed a neuroblastoma proper cDNA microarray (named CCC-NB5000-Chip) carrying 5340 cDNA spots (the 5340 genes system). Insert DNAs (average size, approximately 2.5kb) were amplified by polymerase chain reaction (PCR) from these cDNA clones, purified by ethanol precipitation, and spotted onto a glass slide at a high density with an ink-jet printing tool (NGK Insulators, Ltd.).

Ten micrograms each of total RNA were labeled with the CyScribe RNA labeling kit in accordance with the manufacturer's manual (Amersham Pharmacia Biotech), followed by probe purification with the Qiagen MinElute PCR purification kit (Qiagen). We used a mixture of equal amounts of RNA from each of four neuroblastoma cell lines (NB69, NBL-S, SK-N-AS, and SH-SY5Y) as a reference. RNAs extracted from primary neuroblastoma tissues and RNAs of the reference mixture were labeled with Cy3 and Cy5 dye, respectively, and were used as probes together with yeast tRNA and polyA for suppression. Subsequent hybridization and washing were conducted as described previously (Takahashi et al., 2002; Yoshikawa et al., 2000). Hybridized microarrays were scanned using the Agilent G2505A confocal laser scanner (Agilent Technologies, Inc.), and fluorescent intensities were quantified using the GenePix Pro microarray analysis software (Axon Instruments, Inc.). The procedure of this study was approved by the Institutional Review Board of the Chiba Cancer Center.

After selecting genes strongly related to the prognosis of patients with neuroblastoma (at 2 years and at 5 years after diagnosis), we constructed a 200 cDNAs microarray on glass slides by the same procedure described above (the mini-chip system). For the independent test using 50 samples, tumor RNA preparation, probe labeling, and hybridization were conducted in a completely different laboratory from the original 136 hybridization. In this independent test, 5 μg each of total RNA were used for labeling.

Data preprocessing

To remove chip-wise biases of a microarray system, we used the LOWESS normalization (Cleveland, 1979). When the Cy3 or Cy5 strength for a clone was smaller than 3, strength was regarded as abnormally small, and the log expression ratio of the corresponding clone was treated as a missing value. The rate of such missing entries was less than 1%. After normalizing the 5340 (genes) by 136 (samples) log expression matrix and removing missing values, each missing entry was imputed to an estimated value by Bayesian principal component analysis, which was developed previously (Oba et al., 2003).

Supervised machine learning and LTO crossvalidation

The 96 samples, whose prognosis at 5 years after diagnosis had been successfully checked, were used to train a supervised classifier that predicts the 5 year prognosis of a new patient. When we considered the short-term prediction, 126 samples whose 2 year prognosis is known were used. Selection of the genes that are related to the classification is an important preprocess for reliable prediction. We omitted the genes whose standard

deviation of the log ratios for the genes obtained over 136 experiments was smaller than 0.36, so that 1000 genes remained, because the background noise level was about 0.2–0.3. After the gene screening, the genes were scored by the pairwise *F* score, which is a modification of a pairwise correlation method (Bo and Jonassen, 2002), to conduct gene ranking in an attempt not only to obtain higher discrimination accuracy by using a smaller number of genes but also to reserve the applicability to various outcome prediction by the set of selected genes (see the Supplemental Data).

We used a well-established technique in the supervised classification (prognosis prediction), that is, weighted voting with linear discriminators, where each weight value was calculated as the signal-to-noise ratio (Golub et al., 1999). In the weighted voting, only n genes with the largest pairwise *F* score were used. The number of top genes, n, strongly affects the prediction accuracy (Figure S3) as found in various microarray studies and hence should be determined such to maximize the leave one out (LOO) crossvalidation accuracy. However, a naive determination process of n may introduce information leakage, and the accuracy optimized by the LOO crossvalidation involves overestimation. To avoid such an overestimation, we consulted a LTO analysis. The LTO analysis was constituted of inner and outer loops of LOO (Figure S2A); the gene number n was optimized by the LOO crossvalidation repeating the inner loops, and the optimized classifier was evaluated by an independent test for a single sample left out at a single step in the outer loop. During repetition of such steps, the test results of the outer loop were never fed back to the classifier's optimization process in the inner loops, and hence the tests in the outer loop did not include any overestimation, and the estimated accuracy involved the smallest bias as possible.

The posterior value for a single sample was calculated based on the distribution of the weighted vote (decision by majority by the genes that join the vote) *f* within the LTO analysis. We regard a real-valued weighted vote as carrying two kinds of information: its sign predicts the label (favorable or unfavorable) of the corresponding sample, and its absolute value shows the prediction strength. The posterior probability p for this sample being favorable (alive at 5 years) was evaluated as the logit transformation $p = \exp(\beta_0 + \beta_1 f)/[1 + \exp(\beta_0 + \beta_1 f)]$, where parameters β_0 and β_1 were estimated by the maximum likelihood method, in each step in the outer loop of LTO using the remaining 95 samples and the corresponding labels (5 year prognosis). Then, the posterior probability of the sample left out in the outer loop was predicted by the weighted vote *f* by the classifier constructed in the inner LOO loops and the parameters β_0 and β_1 obtained above. There is therefore no information leakage in this calculation process of the posterior of the sample left out.

Independent test

Using the 50 independent samples, we performed two kinds of tests. The first one is an independent test to validate the classifier obtained by our method and the applicability of our classifier to the mini-chip system, which has been developed as a clinical tool at the bedside (Figure S2B). According to the LTO analysis, the supervised classifier was finally constructed by using all of the 96 training samples measured by the 5340 genes system. This classifier was evaluated by being directly applied to the 50 samples measured by the mini-chip system without any information from measurements by the mini-chip system and the 50 test samples. In this test, tumor RNA preparation, probe labeling, and hybridization were conducted in a completely different laboratory from that for the 5340 genes system. The second one is to validate the LTO analysis to construct a supervised classifier by applying the procedure to the data taken by the mini-chip system.

Survival analysis

The Kaplan-Meier survival analysis was also programmed and used to compare patient survival. To assess the association of selected gene expression with patient clinical outcome, the statistical p and q values were calculated based on the log rank test.

Immunohistochemistry

Immunostaining with the antibody against peripherin protein (Santa Cruz Biotechnology; 1:400) was performed on six human neuroblastoma tumors selected from the surgical pathology file at the Department of Pathology, Aichi Medical University. They were all neuroblastoma (Schwannian stroma–poor) and included three favorable histology tumors (poorly differentiated subtype without *MYCN* amplification [one case]; differentiated subtype without *MYCN* amplification [two cases]) and three unfavorable histology tumors (undifferentiated subtype without *MYCN* amplification [one case]; poorly differentiated subtype with *MYCN* amplification [one case]; poorly differentiated subtype without *MYCN* amplification). All tumor tissues were obtained prior to chemotherapy and irradiation therapy. Four micron thick sections from the formalin-fixed, paraffin-embedded samples of these tumors were treated according to the protocol described previously (Kato et al., 2004). As for the negative controls, normal goat immunoglobulins (1:500 dilution; Vector Laboratories) were applied as the primary antibody.

Supplemental data

The Supplemental Data include Supplemental Experimental Procedures and ten supplemental figures and can be found with this article online at http://www.cancercell.org/cgi/content/full/7/4/337/DC1/.

Acknowledgments

We are grateful to the hospitals and institutions that provided us with surgical specimens (see the Supplemental Data). We also thank Shigeru Sakiyama and John K. Cowell for reading the manuscript; Naohiko Seki, Tsutomu Yoshikawa, and Masaki Kato for their valuable suggestions; and Natsue Kitabayashi, Tomonori Saito, Naoko Sugimitsu, Yuki Nakamura, Naoko Shibano, Emiko Kojima, Hisae Murakami, and Kazumi Yagyu for their technical support. This work was supported in part by a fund from Hisamitsu Pharmaceutical Co., Inc.; by Grants-in-Aid for Scientific Research on Priority Areas (C) "Medical Genome Science" and "Genome Information Science" and for Scientific Research (B) from the Ministry of Education, Culture, Sports, Science and Technology of Japan; and by Grant-in Aid for Cancer Research from the Ministry of Health, Labor and Welfare of Japan.

Received: November 17, 2003
Revised: January 8, 2005
Accepted: March 11, 2005
Published: April 18, 2005

References

Aletta, J.M., Shelanski, M.L., and Greene, L.A. (1989). Phosphorylation of the peripherin 58-kDa neuronal intermediate filament protein. J. Biochem. (Tokyo) *264*, 4619–4627.

Ambros, I.M., and Ambros, P.F. (1995). Schwann cells in neuroblastoma. Eur. J. Cancer *4*, 429–434.

Ambros, I.M., and Ambros, P.F. (2000). The role of Schwann cells in neuroblastoma. In Neuroblastoma, G.M. Brodeur, T. Sawada, Y. Tsuchida, and P.A. Voute, eds. (Amsterdam: Elsevier), pp. 229–243.

Beer, D.G., Kardia, S.L., Huang, C.C., Giordano, T.J., Levin, A.M., Misek, D.E., Lin, L., Chen, G., Gharib, T.G., Thomas, D.G., et al. (2002). Gene-expression profiles predict survival of patients with lung adenocarcinoma. Nat. Med. *8*, 816–824.

Berwanger, B., Hartmann, O., Bergmann, E., Bernard, S., Nielsen, D., Krause, M., Kartal, A., Flynn, D., Wiedemeyer, R., Schwab, M., et al. (2002). Loss of a FYN-regulated differentiation and growth arrest pathway in advanced stage neuroblastoma. Cancer Cell *2*, 377–386.

Bo, T., and Jonassen, I. (2002). New feature subset selection procedures for classification of expression profiles. Genome Biol. *3*, RESEARCH0017.

Bolande, R.P. (1974). The neurocristopathies: a unifying concept of disease arising in neural crest maldevelopment. Hum. Pathol. *5*, 409–429.

Brodeur, G.M., and Nakagawara, A. (1992). Molecular basis for clinical heterogeneity in neuroblastoma. Am. J. Pediatr. Hematol. Oncol. *14*, 111–116.

Brodeur, G.M., Seeger, R.C., Schwab, M., Varmus, H.E., and Bishop, J.M.

(1984). Amplification of N-myc in untreated human neuroblastomas correlates with advanced disease stage. Science *224*, 1121–1124.

Brodeur, G.M., Fong, C.T., Morita, M., Griffith, R., Hayes, F.A., and Seeger, R.C. (1988). Molecular analysis and clinical significance of N-myc amplification and chromosome 1p monosomy in human neuroblastomas. Prog. Clin. Biol. Res. *271*, 3–15.

Brodeur, G.M., Pritchard, J., Berthold, F., Carlsen, N.L., Castel, V., Castelberry, R.P., De Bernardi, B., Evans, A.E., Favrot, M., Hedborg, F., et al. (1993). Revisions of the international criteria for neuroblastoma diagnosis, staging, and response to treatment. J. Clin. Oncol. *11*, 1466–1477.

Ceci, M., Gaviraghi, C., Gorrini, C., Sala, L.A., Offenhauser, N., Marchisio, P.C., and Biffo, S. (2003). Release of eIF6 (p27BBP) from the 60S subunit allows 80S ribosome assembly. Nature *426*, 579–584.

Chomczynski, P., and Sacchi, N. (1987). Single-step method of RNA isolation by acid guanidinium thiocyanate-phenol-chloroform extraction. Anal. Biochem. *162*, 156–159.

Cleveland, W.S. (1979). Robust locally weighted regression and smoothing scatterplots. J. Am. Stat. Assoc. *74*, 829–836.

Evans, A.E., D'Angio, G.J., and Randolph, J. (1971). A proposed staging for children with neuroblastoma. Children's cancer study group A. Cancer *27*, 374–378.

Favrot, M.C., Combaret, V., and Lasset, C. (1993). CD44—a new prognostic marker for neuroblastoma. N. Engl. J. Med. *329*, 1965.

Godbout, R., and Squire, J. (1993). Amplification of a DEAD box protein gene in retinoblastoma cell lines. Proc. Natl. Acad. Sci. USA *90*, 7578–7582.

Golub, T.R., Slonim, D.K., Tamayo, P., Huard, C., Gaasenbeek, M., Mesirov, J.P., Coller, H., Loh, M.L., Downing, J.R., Caligiuri, M.A., et al. (1999). Molecular classification of cancer: class discovery and class prediction by gene expression monitoring. Science *286*, 531–537.

Hall, J.L., and Cowan, N.J. (1985). Structural features and restricted expression of a human α-tubulin gene. Nucleic Acids Res. *13*, 207–223.

Hishiki, T., Nimura, Y., Isogai, E., Kondo, K., Ichimiya, S., Nakamura, Y., Ozaki, T., Sakiyama, S., Hirose, M., Seki, N., et al. (1998). Glial cell line-derived neurotrophic factor/neurturin-induced differentiation and its enhancement by retinoic acid in primary human neuroblastomas expressing c-Ret, GFR α-1, and GFR α-2. Cancer Res. *58*, 2158–2165.

Hiyama, E., Hiyama, K., Yokoyama, T., Matsuura, Y., Piatyszek, M.A., and Shay, J.W. (1995). Correlating telomerase activity levels with human neuroblastoma outcomes. Nat. Med. *1*, 249–255.

Iizuka, N., Oka, M., Yamada-Okabe, H., Nishida, M., Maeda, Y., Mori, N., Takao, T., Tamesa, T., Tangoku, A., Tabuchi, H., et al. (2003). Oligonucleotide microarray for prediction of early intrahepatic recurrence of hepatocellular carcinoma after curative resection. Lancet *361*, 923–929.

Kaneko, M., Nishihira, H., Mugishima, H., Ohnuma, N., Nakada, K., Kawa, K., Fukuzawa, M., Suita, S., Sera, Y., and Tsuchida, Y. (1998). Stratification of treatment of stage 4 neuroblastoma patients based on N-myc amplification status. Study Group of Japan for Treatment of Advanced Neuroblastoma, Tokyo, Japan. Med. Pediatr. Oncol. *31*, 1–7.

Kato, C., Miyazaki, K., Nakagawa, A., Ohira, M., Nakamura, Y., Ozaki, T., Imai, T., and Nakagawara, A. (2004). High expression of human tubulin tyrosine ligase and enhanced tubulin tyrosination/detyrosination cycle are associated with neuronal differentiation in neuroblastomas with favorable prognosis. Int. J. Cancer *112*, 365–375.

Knoops, B., and Octave, J.N. (1997). α1-tubulin mRNA level is increased during neurite outgrowth of NG 108-15 cells but not during neurite outgrowth inhibition by CNS myelin. Neuroreport *8*, 795–798.

Look, A.T., Hayes, F.A., Nitschke, R., McWilliams, N.B., and Green, A.A. (1984). Cellular DNA content as a predictor of response to chemotherapy in infants with unresectable neuroblastoma. N. Engl. J. Med. *311*, 231–235.

Look, A.T., Hayes, F.A., Shuster, J.J., Douglass, E.C., Castleberry, R.P., Bowman, L.C., Smith, E.I., and Brodeur, G.M. (1991). Clinical relevance of tumor cell ploidy and N-myc gene amplification in childhood neuroblastoma: a Pediatric Oncology Group study. J. Clin. Oncol. *9*, 581–591.

Nagata, T., Takahashi, Y., Asai, S., Ishii, Y., Mugishima, H., Suzuki, T., Chin, M., Harada, K., Koshinaga, S., and Ishikawa, K. (2000). The high level of hCDC10 gene expression in neuroblastoma may be associated with favorable characteristics of the tumor. J. Surg. Res. *92*, 267–275.

Nakagawara, A., Arima, M., Azar, C.G., Scavarda, N.J., and Brodeur, G.M. (1992). Inverse relationship between trk expression and N-myc amplification in human neuroblastomas. Cancer Res. *52*, 1364–1368.

Nakagawara, A., Arima-Nakagawara, M., Scavarda, N.J., Azar, C.G., Cantor, A.B., and Brodeur, G.M. (1993). Association between high levels of expression of the TRK gene and favorable outcome in human neuroblastoma. N. Engl. J. Med. *328*, 847–854.

Nakagawara, A., Milbrandt, J., Muramatsu, T., Deuel, T.F., Zhao, H., Cnaan, A., and Brodeur, G.M. (1995). Differential expression of pleiotrophin and midkine in advanced neuroblastomas. Cancer Res. *55*, 1792–1797.

Noguchi, T., Akiyama, K., Yokoyama, M., Kanda, N., Matsunaga, T., and Nishi, Y. (1996). Amplification of a DEAD box gene (DDX1) with the MYCN gene in neuroblastomas as a result of cosegregation of sequences flanking the MYCN locus. Genes Chromosomes Cancer *15*, 129–133.

Ntzani, E.E., and Ioannidis, J.P. (2003). Predictive ability of DNA microarrays for cancer outcomes and correlates: an empirical assessment. Lancet *362*, 1439–1444.

Oba, S., Takemasa, N., Monden, M., Matsubara, K., and Ishii, S. (2003). A Bayesian missing value estimation method. Bioinformatics *19*, 2088–2096.

Ohira, M., Morohashi, A., Inuzuka, H., Shishikura, T., Kawamoto, T., Kageyama, H., Nakamura, Y., Isogai, E., Takayasu, H., Sakiyama, S., et al. (2003a). Expression profiling and characterization of 4200 genes cloned from primary neuroblastomas: identification of 305 genes differentially expressed between favorable and unfavorable subsets. Oncogene *22*, 5525–5536.

Ohira, M., Morohashi, A., Nakamura, Y., Isogai, E., Furuya, K., Hamano, S., Machida, T., Aoyama, M., Fukumura, M., Miyazaki, K., et al. (2003b). Neuroblastoma oligo-capping cDNA project: toward the understanding of the genesis and biology of neuroblastoma. Cancer Lett. *197*, 63–68.

Sawada, T., Hirayama, M., Nakata, T., Takeda, T., Takasugi, N., Mori, T., Maeda, K., Koide, R., Hanawa, Y., Tsunoda, A., et al. (1984). Mass screening for neuroblastoma in infants in Japan. Interim report of a mass screening study group. Lancet *2*, 271–273.

Schwab, M., Alitalo, K., Klempnauer, K.H., Varmus, H.E., Bishop, J.M., Gilbert, F., Brodeur, G., Goldstein, M., and Trent, J. (1983). Amplified DNA with limited homology to myc cellular oncogene is shared by human neuroblastoma cell lines and a neuroblastoma tumour. Nature *305*, 245–248.

Shimada, H., Chatten, J., Newton, W.A., Sachs, N., Hamoudi, A.B., Chiba, T., Marsden, H.B., and Misugi, K. (1984). Histopathologic prognostic factors in neuroblastic tumors; definition of subtypes of ganglioneuroblastoma and an age-linked classification of neuroblastomas. J. Natl. Cancer Inst. *73*, 405–416.

Shimono, R., Matsubara, S., Takamatsu, H., Fukushige, T., and Ozawa, M. (2000). The expression of cadherins in human neuroblastoma cell lines and clinical tumors. Anticancer Res. *20*, 917–923.

Slavc, I., Ellenbogen, R., Jung, W.H., Vawter, G.F., Kretschmar, C., Grier, H., and Korf, B.R. (1990). myc gene amplification and expression in primary human neuroblastoma. Cancer Res. *50*, 1459–1463.

Storey, J.D., and Tibshirani, R. (2003). Statistical significance for genome-wide studies. Proc. Natl. Acad. Sci. USA *100*, 9440–9445.

Takahashi, M., Seki, N., Ozaki, T., Kato, M., Kuno, T., Nakagawa, T., Watanabe, K., Miyazaki, K., Ohira, M., Hayashi, S., et al. (2002). Identification of the p33(ING1)-regulated genes that include cyclin B1 and proto-oncogene DEK by using cDNA microarray in a mouse mammary epithelial cell line NMuMG. Cancer Res. *62*, 2203–2209.

Ueda, K. (2001). Detection of the retinoic acid-regulated genes in a RTBM1 neuroblastoma cell line using cDNA microarray. Kurume Med. J. *48*, 159–164.

van 't Veer, L.J., Dai, H., van de Vijver, M.J., He, Y.D., Hart, A.A., Mao, M., Peterse, H.L., van der Kooy, K., Marton, M.J., Witteveen, A.T., et al. (2002). Gene expression profiling predicts clinical outcome of breast cancer. Nature *415*, 530–536.

Yamanaka, Y., Hamazaki, Y., Sato, Y., Ito, K., Watanabe, K., Heike, T., Nakahata, T., and Nakamura, Y. (2002). Maturational sequence of neuroblastoma revealed by molecular analysis on cDNA microarrays. Int. J. Oncol. *21*, 803–807.

Yoshikawa, T., Nagasugi, Y., Azuma, T., Kato, M., Sugano, S., Hashimoto, K., Masuho, Y., Muramatsu, M., and Seki, N. (2000). Isolation of novel mouse genes differentially expressed in brain using cDNA microarray. Biochem. Biophys. Res. Commun. *275*, 532–537.

Accession numbers

Microarray data are available at NCBI Gene Expression Omnibus (accession number GSE2283).

THE JOURNAL OF BIOLOGICAL CHEMISTRY
Vol. 280, No. 17, Issue of April 29, pp. 16665–16675, 2005
Printed in U.S.A.

Identification of Protein Kinase A Catalytic Subunit β as a Novel Binding Partner of p73 and Regulation of p73 Function*

Received for publication, December 20, 2004, and in revised form, January 31, 2005
Published, JBC Papers in Press, February 21, 2005, DOI 10.1074/jbc.M414323200

Takayuki Hanamoto‡§, Toshinori Ozaki‡, Kazushige Furuya‡, Mitsuchika Hosoda‡, Syunji Hayashi‡, Mitsuru Nakanishi‡, Hideki Yamamoto‡, Hironobu Kikuchi‡, Satoru Todo§, and Akira Nakagawara‡¶

From the ‡Division of Biochemistry, Chiba Cancer Center Research Institute, Chiba 260-8717, Japan and the §Department of General Surgery, Hokkaido University School of Medicine, Kita-ku, Sapporo 060-8638, Japan

Post-translational modifications play a crucial role in regulation of the protein stability and pro-apoptotic function of p53 as well as its close relative p73. Using a yeast two-hybrid screening based on the Sos recruitment system, we identified protein kinase A catalytic subunit β (PKA-Cβ) as a novel binding partner of p73. Co-immunoprecipitation and glutathione *S*-transferase pull-down assays revealed that p73α associated with PKA-Cβ in mammalian cells and that their interaction was mediated by both the N- and C-terminal regions of p73α. In contrast, p53 failed to bind to PKA-Cβ. *In vitro* phosphorylation assay demonstrated that glutathione *S*-transferase-p73α-(1–130), which has one putative PKA phosphorylation site, was phosphorylated by PKA. Enforced expression of PKA-Cβ resulted in significant inhibition of the transactivation function and pro-apoptotic activity of p73α, whereas a kinase-deficient mutant of PKA-Cβ had no detectable effect. Consistent with this notion, treatment with H-89 (an ATP analog that functions as a PKA inhibitor) reversed the dibutyryl cAMP-mediated inhibition of p73α. Of particular interest, PKA-Cβ facilitated the intramolecular interaction of p73α, thereby masking the N-terminal transactivation domain with the C-terminal inhibitory domain. Thus, our findings indicate a PKA-Cβ-mediated inhibitory mechanism of p73 function.

p73 has been identified as a structural and functional homolog of the tumor suppressor p53 (1). p53 and p73 share the same domain organization, consisting of an N-terminal transactivation domain, a central sequence-specific DNA-binding domain, and a C-terminal oligomerization domain. As expected, several pieces of evidence suggest that p73 can bind to the p53-responsive element and transactivate an overlapping set of p53 target genes, thus leading to induction of G_1/S cell cycle arrest and apoptosis (1–6). In marked contrast to p53, p73 is expressed as multiple isoforms arising from alternative splicing of the primary p73 transcript (p73α, p73β, p73γ, p73δ, p73ε, p73η, and p73ζ) termed the TA variant (1, 3, 7–9). These alternatively spliced isoforms vary in their C termini and display different transcriptional and biological properties. Additionally, the ΔN variant (ΔNp73α and ΔNp73β), which is generated by alternative promoter utilization, lacks the N-terminal transactivation domain and exhibits dominant-negative behavior toward wild-type p73 as well as p53 (10–12). Recently, we (14) and others (13, 15) demonstrated that p73 directly transactivates the expression of its own negative regulator (ΔNp73), creating an autoregulatory feedback loop in which both the activity of p73 and the expression of ΔNp73 are regulated. Thus, the pro-apoptotic activity of p73 is determined by the relative expression levels of its TAp73 and dominant-negative ΔNp73 variants in cells.

In sharp contrast to p53, it was initially reported that p73 was not induced by DNA damage (1). However, recent studies demonstrated that, in response to a subset of DNA-damaging agents, p73 is positively regulated by multiple post-translational modifications, including phosphorylation and acetylation. During cisplatin-mediated apoptosis, phosphorylation of p73 at Tyr-99 by the non-receptor tyrosine kinase c-Abl results in an increase in its stability and pro-apoptotic activity (16–18). In addition to c-Abl, the protein kinase Cδ catalytic fragment has the ability to phosphorylate p73 at Ser-289 and contributes to the accumulation of p73 during the apoptotic response to cisplatin treatment (19). It is worth noting that the physical and functional interaction between c-Abl and protein kinase Cδ leads to the cross-activation of their kinase functions (20, 21). Furthermore, the enzymatic activity of Chk1 (checkpoint kinase-1) is enhanced in response to DNA damage (22–24), and Chk1 has the ability to phosphorylate p73 at Ser-47 upon DNA damage, thereby enhancing its transactivation ability and pro-apoptotic activity without affecting the level of total p73 protein, whereas Chk2 has no detectable effect on p73 (25). Alternatively, Zeng *et al.* (26) found that the acetyltransferase p300/CBP (cAMP-responsive element-binding protein-binding protein) interacts with the N-terminal region of p73 and stimulates p73-mediated transcriptional activation and apoptosis. Recently, Costanzo *et al.* (27) reported that doxorubicin treatment induces the p300-mediated acetylation of p73 at Lys-321, Lys-327, and Lys-331 in a c-Abl-dependent manner, which is associated with the efficient recruitment of p73 to the promoter of the apoptotic target gene *p53AIP1*. Additionally, it has been shown that p300-mediated acetylation of p73 results in its significant stabilization in a prolyl isomerase Pin1-dependent manner (28).

To identify cellular protein(s) that could interact with full-length p73α and regulate its function, we screened a human fetal brain cDNA library using a yeast two-hybrid method

* This work was supported in part by a grant-in-aid from the Ministry of Health, Labor, and Welfare for Third Term Comprehensive Control Research for Cancer; a grant-in-aid for scientific research on priority areas from the Ministry of Education, Culture, Sports, Science, and Technology of Japan; and a grant-in-aid for scientific research from the Japan Society for the Promotion of Science. The costs of publication of this article were defrayed in part by the payment of page charges. This article must therefore be hereby marked "*advertisement*" in accordance with 18 U.S.C. Section 1734 solely to indicate this fact.

¶ To whom correspondence should be addressed: Div. of Biochemistry, Chiba Cancer Center Research Inst., 666-2 Nitona, Chuoh-ku, Chiba 260-8717, Japan. Tel.: 81-43-264-5431; Fax: 81-43-265-4459; E-mail: akiranak@chiba-cc.jp.

based on the Sos recruitment system. We report here that protein kinase A catalytic subunit β (PKA-Cβ)[1] bound to p73α in cells, but not to p53, and that their interaction was mediated by the N- and C-terminal regions of p73α. *In vitro* kinase assays revealed that the catalytic subunit of PKA phosphorylated p73α. PKA-Cβ inhibited the p73α-mediated transcriptional activation of the $p21^{WAF1}$ and *Bax* promoters and p73α-dependent apoptosis in response to camptothecin. On the other hand, the kinase-deficient mutant of PKA-Cβ had little effect on p73α. Of note, we found that PKA-Cβ facilitated the intramolecular interaction of p73α. Our results strongly suggest the PKA-Cβ-mediated phosphorylation and intramolecular interaction of p73 to be a novel inhibitory mechanism of p73 function.

EXPERIMENTAL PROCEDURES

Cell Culture and Cell Lines—SV40-transformed African green monkey kidney cells (COS-7) were grown in Dulbecco's modified Eagle's medium supplemented with 10% heat-incubated fetal bovine serum (Invitrogen), 100 IU/ml penicillin, and 100 μg/ml streptomycin. p53-deficient human lung carcinoma H1299 cells were maintained in RPMI 1640 medium supplemented with 10% heat-incubated fetal bovine serum and antibiotic mixture. The cells were cultured at 37 °C in a water-saturated atmosphere of 95% air and 5% CO_2.

Transient Transfection—COS-7 cells grown to 50–70% confluence in 60-mm dishes were transfected with the indicated expression plasmids using FuGENE 6 transfection reagent (Roche Applied Science) following the protocol recommended by the manufacturer. H1299 cells transfection was performed using Lipofectamine 2000 transfection reagent (Invitrogen) according to the manufacturer's instructions.

Yeast Two-hybrid Screening—The CytoTrap two-hybrid system was purchased from Stratagene (La Jolla, CA). The cDNA encoding the full-length open reading frame of human p73α was amplified by PCR using pcDNA3-p73α as template. The PCR product, which was produced by additional upstream 5′-BamHI and downstream 3′-SalI restriction sites, was digested completely with BamHI and SalI; purified on agarose gel; and directly inserted in-frame into the identical restriction sites of pSos to give pSos-p73α. The resulting pSos-p73α"bait" plasmid was used to identify the cDNA encoding the p73α-binding protein from a human fetal brain cDNA library cloned into the pMyr plasmid (Stratagene). The screening was carried out according to the manufacturer's instructions. Briefly, a temperature-sensitive yeast strain (cdc25Hα) was cotransformed with pSos-p73α and the cDNA library using the lithium acetate/heat shock procedure as described previously (29). Transformants were allowed to grow on selection medium containing glucose for 2 days at 25 °C and then transferred onto selection medium containing galactose. Plasmid DNAs were isolated from the colonies exhibiting galactose-dependent growth at 37 °C and transformed into *Escherichia coli*. Finally, the nucleotide sequences of the positive cDNA clones were determined by the dideoxy terminator cycle sequencing using an ABI automated DNA sequencer (Applied Biosystems, Foster City, CA).

Western Blot Analysis—Transfected cells were washed twice with phosphate-buffered saline (PBS) and lysed in ice-cold lysis buffer A (25 mM Tris-Cl (pH 7.5), 137 mM NaCl, 2.7 mM KCl, and 1% Triton X-100) containing protease inhibitor mixture (Sigma). After a brief sonication, whole cell lysates were centrifuged at 15,000 rpm for 10 min at 4 °C to remove insoluble materials, and the protein concentrations of the supernatants were determined using the Bio-Rad protein assay reagent. Protein samples were boiled in SDS sample buffer for 5 min, resolved by 10% SDS-PAGE, and transferred onto Immobilon-P membranes (Millipore, Bedford, MA). The membranes were blocked overnight with 50 mM Tris-Cl (pH 7.6), 100 mM NaCl, and 0.1% Tween 20 containing 5% nonfat dry milk and then incubated at room temperature for 1 h with anti-FLAG monoclonal antibody (M2, Sigma), anti-green fluorescence protein (GFP) monoclonal antibody (1E4, Medical and Biological Laboratories, Nagoya, Japan), anti-p53 monoclonal antibody (DO-1, Oncogene Research Products, Cambridge, MA), anti-p73 monoclonal antibody (Ab-4, NeoMarkers, Inc., Fremont, CA), anti-$p21^{WAF1}$ monoclonal antibody (Ab-1, Oncogene Research Products), anti-PKA-Cα polyclonal antibody (C-20, Santa Cruz Biotechnology, Inc., Santa Cruz, CA), or anti-PKA-Cβ polyclonal antibody (C-20, Santa Cruz Biotechnology, Inc.), followed by incubation with the corresponding horseradish peroxidase-conjugated secondary antibodies (Jackson ImmunoResearch Laboratories, Inc., West Grove, PA). Following the last wash, horseradish peroxidase-labeled antibodies were detected using an enhanced chemiluminescence detection system (ECL, Amersham Biosciences) according to the manufacturer's instructions.

Immunoprecipitation and Pull-down Assay—For immunoprecipitation, cell lysates were prepared in lysis buffer A. Equal amounts of protein extracts were pre-absorbed with protein G-Sepharose beads (Amersham Biosciences) for 1 h at 4 °C, and the precleared lysates were incubated with the indicated antibodies for 2 h at 4 °C, followed by incubation with protein G-Sepharose beads for an additional 1 h at 4 °C. The immune complexes were then washed three times with lysis buffer A, eluted by boiling in SDS sample buffer for 5 min, and subjected to Western blot analysis. For glutathione *S*-transferase (GST) pull-down assays, GST alone or the indicated GST-p73α fusion proteins were expressed in *E. coli* strain DH5α and loaded onto glutathione-Sepharose 4B beads (Amersham Biosciences). PKA-Cβ was generated *in vitro* in the presence of [^{35}S]methionine using the TNT quick-coupled *in vitro* transcription/translation system (Promega Corp., Madison, WI) according to the manufacturer's instructions. ^{35}S-Labeled PKA-Cβ was incubated with GST or GST-p73α fusion proteins bound to glutathione-Sepharose beads for 2 h at 4 °C in a total volume of 400 μl of binding buffer (50 mM Tris-Cl (pH 7.5), 150 mM NaCl, and 0.1% Nonidet P-40). Beads were washed extensively with the same buffer, and the radiolabeled proteins were eluted by boiling in SDS sample buffer for 5 min. Following electrophoresis, gels were destained, dried, and exposed to an x-ray film with an intensifying screen at −80 °C.

Cell Fractionation—Transfected COS-7 cells were fractionated into nuclear and cytoplasmic fractions as described previously (30). In brief, cells were washed twice with ice-cold 1× PBS and lysed in lysis buffer B containing 10 mM Tris-Cl (pH 7.5), 1 mM EDTA, 0.5% Nonidet P-40, and protease inhibitor mixture for 30 min at 4 °C. Cell lysates were centrifuged at 15,000 rpm for 10 min at 4 °C to separate soluble (cytoplasmic) from insoluble (nuclear) fractions. The pellets were washed extensively with lysis buffer B and further dissolved in 1× SDS sample buffer. The nuclear and cytoplasmic fractions were analyzed by immunoblotting with anti-lamin B monoclonal antibody (Ab-1, Oncogene Research Products) or with anti-α-tubulin monoclonal antibody (Ab-2, NeoMarkers, Inc.).

Immunofluorescence Microscopy—H1299 cells were grown on coverslips and transiently cotransfected with the expression plasmids for hemagglutinin (HA)-p73α and FLAG-PKA-Cβ. Forty-eight hours after transfection, cells were fixed with 3.7% formaldehyde in PBS for 30 min at room temperature and permeabilized with 0.2% Triton X-100 for 5 min. Nonspecific binding sites were blocked by treating cells with PBS containing 3% bovine serum albumin. The cells were incubated with anti-HA polyclonal and anti-FLAG monoclonal antibodies for 1 h, followed by incubation with fluorescein isothiocyanate- and rhodamine-conjugated secondary antibodies (Invitrogen). The coverslips were washed with PBS, mounted onto slides, and observed under a Fluoview laser scanning confocal microscope (Olympus, Tokyo, Japan).

Luciferase Reporter Assay—p53-deficient H1299 cells (5×10^4 cells in a 12-well plate) were transiently cotransfected with a constant amount of the indicated expression plasmid (HA-p73α, HA-p73β, or p53), a p53/p73-responsive luciferase reporter construct ($p21^{WAF1}$ or *bax*), and pRL-TK encoding *Renilla* luciferase with or without increasing amounts of the expression plasmid for FLAG-PKA-Cβ. The total amount of DNA was kept constant (510 ng) with pcDNA3 per transfection. Forty-eight hours after transfection, cells were lysed and assayed for luciferase activity using the Dual-Luciferase reporter assay system (Promega Corp.) according to the manufacturer's recommendations. The transfection efficiency was normalized based on pRL-TK reporter activity.

Reverse Transcription-PCR—H1299 cells were transiently cotransfected with the indicated combinations of expression plasmids. Twenty-four hours after transfection, total RNA was prepared using an RNeasy mini kit (Qiagen Inc.) according to the manufacturer's protocol. One microgram of total RNA was used to synthesize the first-strand cDNA using random primers and SuperScript II reverse transcriptase (Invitrogen). Reverse transcription was carried out at 42 °C for 90 min, and reverse transcripts were amplified by standard PCR with *rTaq* DNA polymerase (Takara, Ohtsu, Japan). The primers used for PCR were as follows: $p21^{WAF1}$, 5′-ATGAAATTCACCCCCTTTCC-3′ (sense) and 5′-CCCTAGGCTGTGCTCACTTC-3′ (antisense); and glyceraldehyde-3-phosphate dehydrogenase, 5′-ACCTGACCTGCCGTCTAGAA-3′

[1] The abbreviations used are: PKA-C, protein kinase A catalytic subunit; PBS, phosphate-buffered saline; GFP, green fluorescence protein; GST, glutathione *S*-transferase; HA, hemagglutinin; ChIP, chromatin immunoprecipitation; Bt_2cAMP, dibutyryl cAMP.

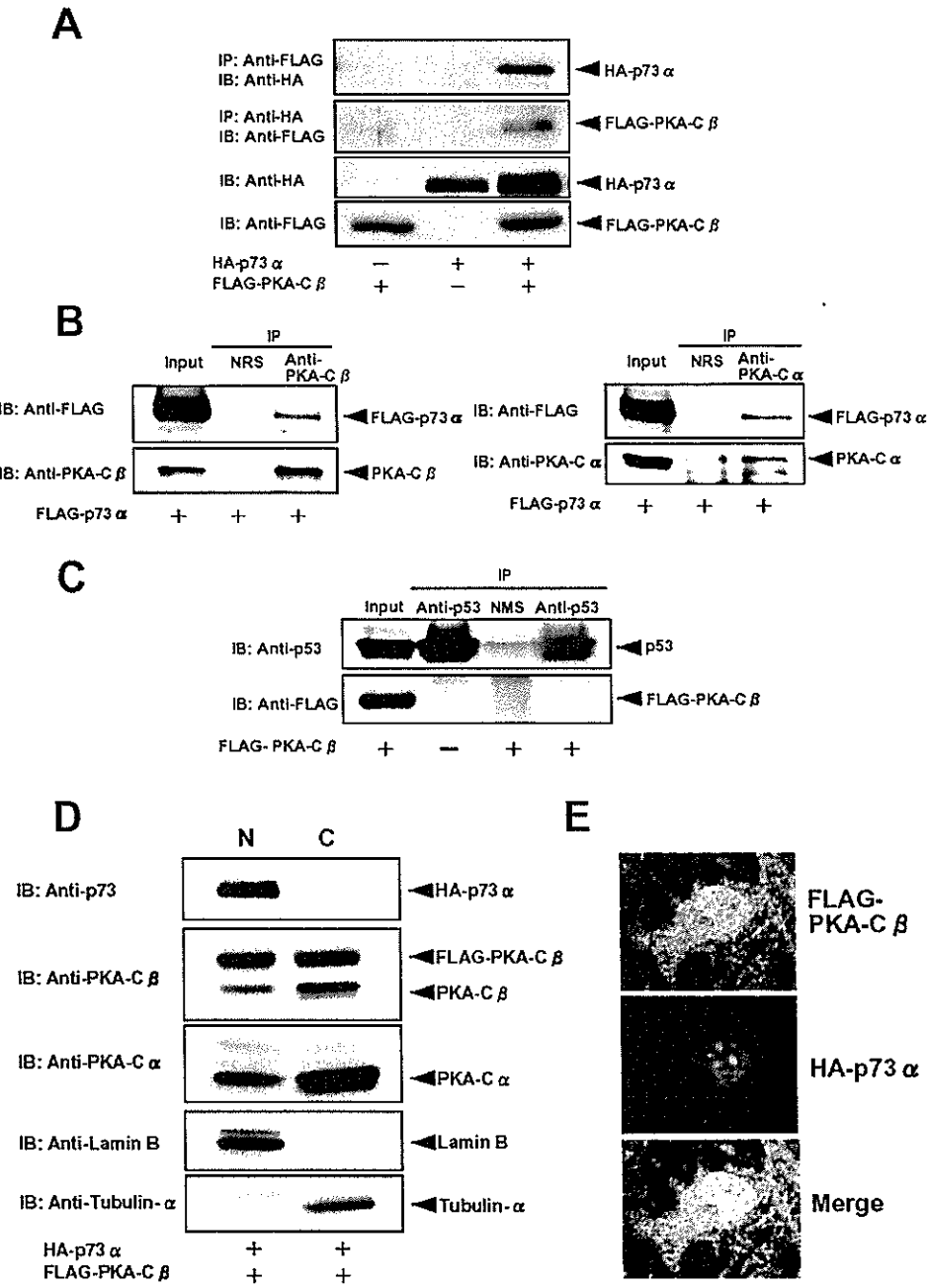

FIG. 1. **Interaction between p73 and PKA-Cβ in mammalian cultured cells.** *A*, p73α forms a complex with PKA-Cβ in COS-7 cells. Whole cell lysates prepared from COS-7 cells transiently cotransfected with the indicated combinations of expression plasmids were immunoprecipitated (*IP*) with anti-FLAG or anti-HA monoclonal antibody. Immunoprecipitates were analyzed by immunoblotting (*IB*) with anti-HA (*first panel*) or anti-FLAG (*second panel*) monoclonal antibody. Whole cell lysates were immunoblotted with anti-HA (*third panel*) or anti-FLAG (*fourth panel*) monoclonal antibody to show the expression of HA-p73α or FLAG-PKA-Cβ, respectively. *B*, p73α binds to endogenous PKA-C in COS-7 cells. COS-7 cells were transiently transfected with the expression plasmid for FLAG-p73α. Forty-eight hours after transfection, whole cell lysates were prepared and subjected to immunoprecipitation with anti-PKA-Cβ (*left panels*) or anti-PKA-Cα (*right panels*) polyclonal antibody. Immunoprecipitation with normal rabbit serum (*NRS*) was used as a negative control. After immunoprecipitation, coprecipitating FLAG-p73α was detected by immunoblotting with anti-FLAG monoclonal antibody. *C*, PKA-Cβ does not bind to endogenous p53. COS-7 cells were transiently transfected with the empty control plasmid or with the expression plasmid encoding FLAG-PKA-Cβ. Forty-eight hours post-transfection, whole cell lysates were prepared and subjected to immunoprecipitation with anti-p53 monoclonal antibody or normal mouse serum (*NMS*), followed by immunoblotting with anti-p53 (*upper panel*) or anti-FLAG (*lower panel*) monoclonal antibody. *D*, subcellular localization of exogenous and endogenous PKA-Cβ. p53-deficient H1299 cells were transiently cotransfected with the expression plasmids for HA-p73α and FLAG-PKA-Cβ (*first* through *third panels*). Forty-eight hours after transfection, transfected cells were fractionated into nuclear (*N*) and cytoplasmic (*C*) fractions as described under "Experimental Procedures." Each fraction was adjusted to an equal volume, and the aliquots of these fractions were separated by 10% SDS-PAGE, followed by immunoblotting with the indicated antibodies. These fractions were analyzed for lamin B (*fourth panel*) and α-tubulin (*fifth panel*) to show the validity of our fractionation technique. *E*, nuclear co-localization of p73 and PKA-Cβ. H1299 cells plated on coverslips were cotransfected with the expression plasmids for HA-p73α and FLAG-PKA-Cβ and processed for immunocytochemical detection using anti-HA and anti-FLAG antibodies. The merged image shows the nuclear co-localization of p73α and PKA-Cβ.

(sense) and 5′-TCCACCACCCTGTTGCTGTA-3′ (antisense). PCR products were separated by 1.5% agarose gel electrophoresis and stained with ethidium bromide.

In Vitro Kinase Assays—GST or the indicated GST-p73α fusion proteins bound to glutathione-Sepharose beads were washed three times with kinase buffer (20 mM Tris-Cl (pH 7.5), 100 mM NaCl, and 12 mM $MgCl_2$). The washed beads were incubated with 30 μl of kinase buffer containing 2 units of purified PKA catalytic subunit (Sigma), 2 mM

dithiothreitol, and 10 μCi of [γ-^{32}P]ATP for 30 min at 4 °C. The reaction mixtures were boiled in 2× SDS sample buffer for 5 min, and the proteins were separated by 10% SDS-PAGE. The gels were dried and processed for autoradiography.

Cell Survival Assays—H1299 cells were seeded in 6-well plates and allowed to attach. Cells were then cotransfected with the indicated expression plasmids. Twenty-four hours after transfection, cells were exposed to camptothecin (final concentration of 1 μM) for 24 h. Cell viability was measured by a colorimetric assay with modified 3-(4,5-dimethylthiazol-2-yl)-2,5-diphenyltetrazolium bromide as the substrate.

Construction of a Kinase-deficient Mutant of PKA-Cβ—The K76R mutation was introduced into wild-type PKA-Cβ by PCR-based mutagenesis using *PfuUltra*™ high fidelity DNA polymerase (Stratagene) according to the manufacturer's protocol. The following oligonucleotide primers were used: 5′-AGGATCTTAGATAAGCAGAAGGTT-3′ (the underlined segment encodes Arg at position 76) and 5′-CATGGCATAATACTGTTCAGTGGCT-3′. This yielded the expression plasmid pcDNA3-FLAG-PKA-Cβ(K76R), which was completely sequenced by the dideoxy chain termination method.

Chromatin Immunoprecipitation (ChIP)—ChIP assays were performed following a protocol provided by Upstate Biotechnology, Inc. (Lake Placid, NY). In brief, H1299 cells were transiently cotransfected with the expression plasmids for HA-p73α (1.2 μg) and FLAG-PKA-Cβ (4.8 μg). Thirty-six hours after transfection, cells were cross-linked with 1% formaldehyde in medium for 15 min at 37 °C. Cells were then washed with ice-cold PBS and resuspended in 200 μl of SDS-sample buffer containing protease inhibitor mixture. The suspension was sonicated 10 times for 30 s with a 1-min cooling period on ice between times and precleared with 20 μl of protein A-agarose beads blocked with sonicated salmon sperm DNA for 30 min at 4 °C. The beads were removed, and the chromatin solution was immunoprecipitated overnight with anti-HA monoclonal antibody at 4 °C, followed by incubation with protein A-agarose beads for an additional 1 h at 4 °C. The immune complexes were eluted with 100 μl of elution buffer (1% SDS and 0.1 M $NaHCO_3$) and formaldehyde cross-links were reversed by heating at 65 °C for 6 h. Proteinase K was added to the reaction mixtures and incubated at 45 °C for 1 h. DNAs of the immunoprecipitates and control input DNAs were purified using a QIAquick PCR purification kit (Qiagen Inc.) and then analyzed by regular PCR using the human p21^{WAF1} and *bax* promoter-specific primers. The primer sequences were 5′-CACCTTTCACCATTCCCCTA-3′ and 5′-GCAGCCCAAGGACAAAATAG-3′ for p21^{WAF1} and 5′-AAAGCTCAGAGGCCCAAAAT-3′ and 5′-AGGCTGAGACGGGGTTATCT-3′ for *bax*.

RESULTS

Identification of PKA-Cβ as a Novel Binding Partner of p73—Because the conventional yeast two-hybrid system depends on the DNA binding as well as the transactivation function of Gal4, it is quite difficult to use a full-length transcriptional regulator with a transactivation domain as bait. To identify potential p73-interacting cellular protein(s), we used full-length p73α as bait in a new CytoTrap yeast two-hybrid screen relying on the Sos recruitment system. A temperature-sensitive yeast strain (cdc25Hα) was cotransformed with a bait plasmid and a human fetal brain cDNA library. Of a total of 1 × 10^6 primary transformants grown on medium containing glucose at 30 °C, one clone (termed F115) exhibited galactose-dependent growth at 37 °C. The plasmid DNA derived from the cDNA library was introduced into *E. coli*, and its nucleotide sequence was determined. Sequence analysis revealed that the F115 cDNA clone encodes full-length PKA-Cβ. Of the PKA catalytic subunit isoforms (PKA-Cα, PKA-Cβ, and PKA-Cγ), PKA-Cβ is highly expressed in brain and reproductive tissues, whereas PKA-Cα is ubiquitously expressed in mammalian tissues (31, 32).

PKA-Cβ Associates with p73 in Mammalian Cultured Cells—To confirm the interaction between PKA-Cβ and p73 detected by the CytoTrap yeast two-hybrid system, co-immunoprecipitation experiments were carried out using whole cell lysates prepared from COS-7 cells expressing exogenous FLAG-PKA-Cβ and HA-p73α. As shown in Fig. 1A, the anti-FLAG immunoprecipitates contained HA-p73α. Used as a control, HA-p73α was not detectable in the anti-FLAG immunoprecipitates of COS-7 cells expressing FLAG-PKA-Cβ or HA-p73α alone. Analysis of the anti-HA immunoprecipitates also demonstrated that FLAG-PKA-Cβ co-immunoprecipitated with HA-p73α. Next, we examined whether endogenous PKA-Cβ could interact with p73α. To this end, whole cell lysates prepared from COS-7 cells transfected with the expression plasmid for FLAG-p73α were immunoprecipitated with normal rabbit serum or with the specific antibody against PKA-Cβ, followed by immunoblotting with anti-FLAG anti-

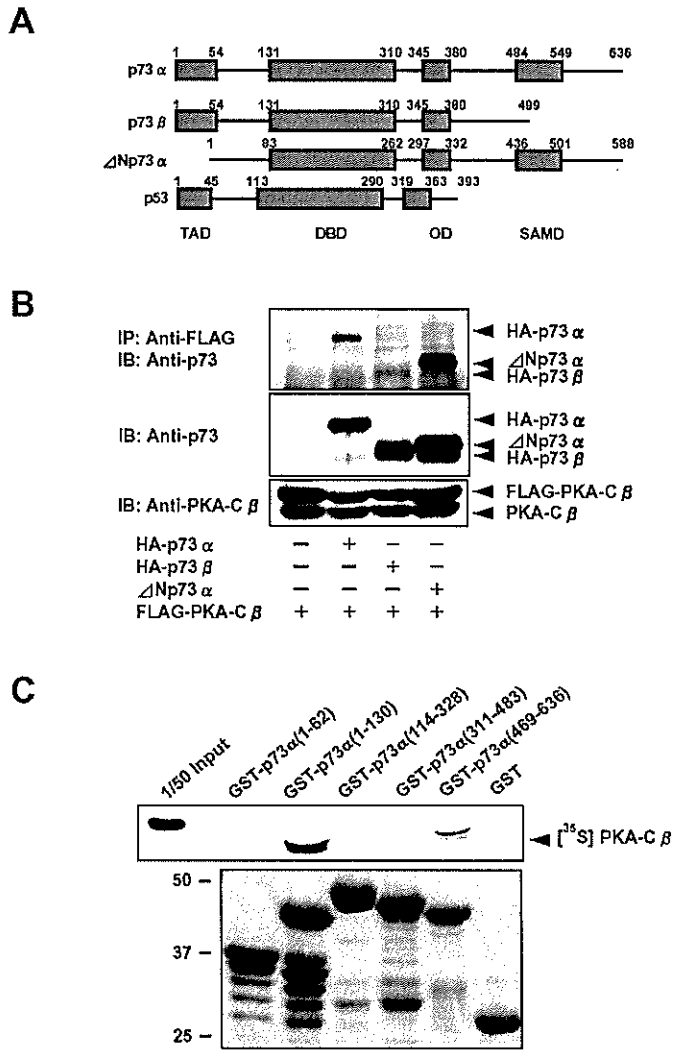

FIG. 2. **Interacting region within p73 for PKA-Cβ.** *A*, domain structures of p73 and p53. The transactivation domain (*TAD*), DNA-binding domain (*DBD*), oligomerization domain (*OD*), and sterile α motif domain (*SAMD*) are indicated. The *numbers* above the p73 variants and p53 indicate amino acid numbering. *B*, interaction of PKA-Cβ with various p73 variants. Whole cell lysates prepared from H1299 cells transiently cotransfected with the expression plasmid for HA-p73α, HA-p73β, or ΔNp73α and with the expression plasmid for FLAG-PKA-Cβ were immunoprecipitated (*IP*) with anti-FLAG monoclonal antibody. The immune complexes were analyzed by immunoblotting (*IB*) with anti-p73 monoclonal antibody (*upper panel*). The expression levels of p73 variants (*middle panel*) and PKA-Cβ (*lower panel*) in whole cell lysates were monitored by immunoblotting with the indicated antibodies. *C*, *in vitro* GST pull-down assays. Bacterially expressed GST or the indicated GST-p73α fusion proteins were incubated with *in vitro* translated ^{35}S-labeled FLAG-PKA-Cβ and precipitated with glutathione-Sepharose 4B beads (50% slurry). After extensive washing, the bound proteins were separated by 10% SDS-PAGE and processed for autoradiography (*upper panel*). *1/50 Input* indicates the radiolabeled FLAG-PKA-Cβ used for *in vitro* pull-down assays that was directly loaded on the same gel as a control. GST and GST-p73α fusion proteins were stained with Coomassie Brilliant Blue (*lower panel*). The positions of molecular mass markers are indicated on the left in kilodaltons.

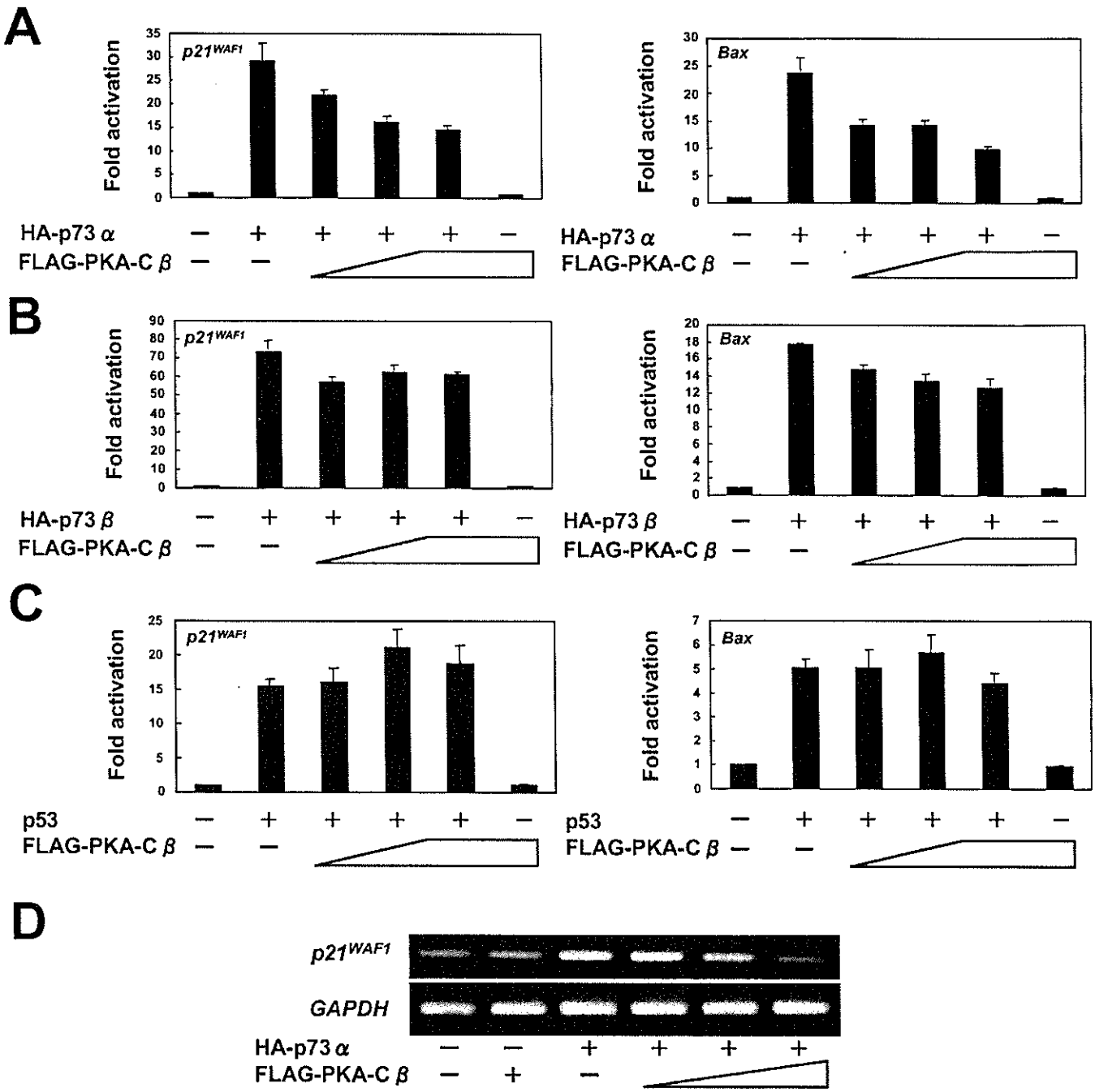

FIG. 3. **PKA-Cβ inhibits p73α-mediated transcriptional activation.** *A–C*, luciferase reporter assays. H1299 cells (5×10^4 cells/12-well plates) were transiently cotransfected with 25 ng of the expression plasmid for HA-p73α (*A*), HA-p73β (*B*), or p53 (*C*); 100 ng of the luciferase reporter construct containing the p53/p73-responsive element derived from the $p21^{WAF1}$ (*left panels*) or *bax* (*right panels*) promoter; and 10 ng of *Renilla* luciferase plasmid (pRL-TK) with or without increasing amounts of the expression plasmid for FLAG-PKA-Cβ (25, 50, and 100 ng). The total amount of the plasmid DNA per transfection was kept constant (510 ng) with pcDNA3. All transfections were performed in triplicate. Luciferase activity was measured 48 h post-transfection. The transfection efficiency was standardized for *Renilla* luciferase activity. The -fold increase in luciferase activity is compared with that in cells transfected with pcDNA3 alone. *D*, reverse transcription-PCR analysis. Total RNA prepared from H1299 cells transiently cotransfected with a constant amount of the expression plasmid for HA-p73α (200 ng) with or without increasing amounts of the expression plasmid for FLAG-PKA-Cβ (200, 400, and 800 ng) was subjected to reverse transcription-PCR analysis for endogenous $p21^{WAF1}$ mRNA expression (*upper panel*). Glyceraldehyde-3-phosphate dehydrogenase (*GAPDH*) mRNA expression levels were used as an internal control (*lower panel*).

body. As shown in Fig. 1*B* (*upper panels*), FLAG-p73α co-immunoprecipitated with endogenous PKA-Cβ. Because the amino acid sequences of PKA-Cα and PKA-Cβ are 91% identical (31), we examined whether endogenous PKA-Cα could bind to p73α. Co-immunoprecipitation experiments revealed that, like PKA-Cβ, endogenous PKA-Cα associated with FLAG-p73α (Fig. 1*B*, *lower panels*). In sharp contrast to p73α, p53 failed to interact with FLAG-PKA-Cβ under our experimental conditions (Fig. 1*C*).

To investigate the subcellular distribution of PKA-Cβ in the presence of exogenous p73α, we employed the biochemical fractionation of transfected H1299 cells. H1299 cells transiently cotransfected with the expression plasmids for HA-p73α and FLAG-PKA-Cβ were fractionated into nuclear and cytoplasmic fractions, and the fractions obtained were subjected to immunoblotting with the indicated antibodies. The purity of the nuclear and cytoplasmic fractions was verified by immunoblotting with anti-lamin B and anti-α-tubulin antibodies, respec-

tively. As shown in Fig. 1*D*, HA-p73α was detected exclusively in the nuclear fractions, whereas FLAG-PKA-Cβ and endogenous PKA-Cβ and PKA-Cα were present in both the cytoplasmic and nuclear fractions. As expected, confocal microscopy of immunostained H1299 cells expressing FLAG-PKA-Cβ and HA-p73α revealed that both proteins co-localized in the cell nucleus (Fig. 1*E*).

Identification of the Interacting Region within p73—To examine which region(s) of p73 could be engaged in the interaction with PKA-Cβ, we performed co-immunoprecipitation and GST pull-down experiments. Fig. 2*A* depicts the domain structures of various p73 variants used for co-immunoprecipitation experiments. Whole cell lysates prepared from H1299 cells transiently cotransfected with the indicated combinations of expression plasmids were immunoprecipitated with anti-FLAG antibody, followed by immunoblotting with anti-p73 antibody. As shown in Fig. 2*B*, HA-p73α and ΔNp73α co-purified with FLAG-PKA-Cβ, whereas the binding of HA-p73β to FLAG-PKA-Cβ was significantly weaker than seen with HA-p73α and ΔNp73α, suggesting that the C-terminal region of p73α might be required for the interaction with PKA-Cβ. To verify these results, *in vitro* GST pull-down assays were carried out using a series of GST-p73α fusion proteins. *In vitro* translated ^{35}S-labeled FLAG-PKA-Cβ was incubated with glutathione-Sepharose beads complexed either with GST alone or with GST-p73α. The autoradiogram in Fig. 2*C* (*upper panel*) shows that GST-p73α-(1–130) and GST-p73α-(469–636) were able to interact with FLAG-PKA-Cβ. The Coomassie Brilliant Blue staining shown in Fig. 2*C* (*lower panel*) revealed that the glutathione-Sepharose beads contained equal amounts of GST-p73α fusion proteins. Taken together, our results suggest that both the N-terminal (amino acids 63–130) and C-terminal (amino acids 469–636) regions of p73α might be essential for the interaction with PKA-Cβ.

PKA-Cβ Inhibits p73α-mediated Transcriptional Activation—In view of the ability of PKA-Cβ to interact with p73α, we next examined whether PKA-Cβ could affect p73α function as a transcriptional regulator. For this purpose, p53-deficient H1299 cells were transiently cotransfected with a constant amount of the expression plasmid for HA-p73α, HA-p73β, or p53 together with the luciferase reporter construct controlled by the p53/p73-responsive element from the p21^{WAF1} or *bax* promoter in the presence or absence of increasing amounts of the expression plasmid for FLAG-PKA-Cβ. All cotransfections included pRL-TK to monitor transfection efficiency, and controls included cotransfections with the empty control plasmid. As shown in Fig. 3*A*, coexpression of FLAG-PKA-Cβ and HA-p73α resulted in marked repression of the p21^{WAF1}- and *bax*-luciferase activities induced by HA-p73α in a dose-dependent manner, and FLAG-PKA-Cβ alone had no effect on the reporter gene activity. In contrast, FLAG-PKA-Cβ had no obvious effects on p73β- and p53-mediated transcriptional activation (Fig. 3, *B* and *C*). These results strongly suggest that there is a correlation between the capacity of PKA-Cβ to interact with p73 or p53 and its ability to inhibit their transactivation function. To determine whether PKA-Cβ could inhibit the p73α-mediated transcriptional activation of endogenous p21^{WAF1}, we performed reverse transcription-PCR analysis using total RNA prepared from H1299 cells transiently cotransfected with the indicated combinations of expression plasmids. As shown in Fig. 3*D*, ectopic expression of HA-p73α resulted in a remarkable up-regulation of endogenous p21^{WAF1} expression, and coexpression of FLAG-PKA-Cβ and HA-p73α inhibited the p73α-mediated induction of p21^{WAF1} in a dose-dependent manner.

To further confirm the inhibitory effect of PKA-Cβ on the transcriptional activity of p73α, H1299 cells were transiently

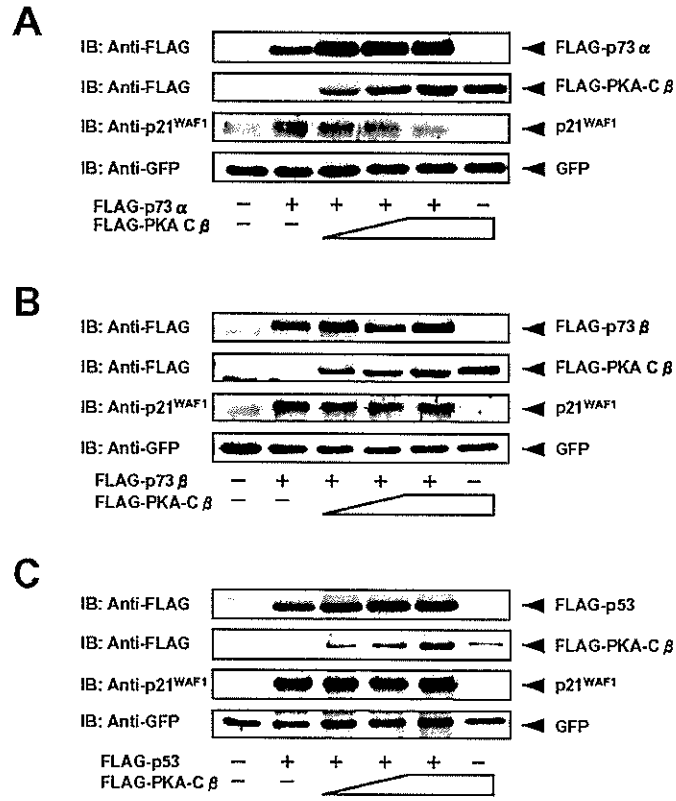

FIG. 4. **PKA-Cβ inhibits the p73α-dependent accumulation of endogenous p21^{WAF1}.** H1299 cells were transiently cotransfected with 200 ng of the expression plasmid for FLAG-p73α (*A*), FLAG-p73β (*B*), or FLAG-p53 (*C*) and 50 ng of the GFP expression plasmid with or without increasing amounts of the expression plasmid for FLAG-PKA-Cβ (200, 400, and 800 ng). Thirty-six hours after transfection, whole cell lysates were prepared and subjected to immunoblotting (*IB*) with the indicated antibodies (*first* through *third panels*). The GFP expression plasmid was included in each transfection as a transfection efficiency control, and the expression levels of GFP were detected with anti-GFP monoclonal antibody (*fourth panels*).

cotransfected with a constant amount of the expression plasmid for FLAG-p73α, FLAG-p73β, or FLAG-p53 with or without increasing amounts of the expression plasmid for FLAG-PKA-Cβ, and the protein levels of endogenous p21^{WAF1} were determined by immunoblotting. As shown in Fig. 4*A*, endogenous p21^{WAF1} was increased by ectopic FLAG-p73α expression, whereas overexpression of FLAG-PKA-Cβ resulted in a reduction in the level of endogenous p21^{WAF1} induced by FLAG-p73α, supporting the notion that PKA-Cβ inhibits the transcriptional activity of p73α. In contrast, PKA-Cβ had no detectable effects on the p73β- or p53-dependent induction of endogenous p21^{WAF1} (Fig. 4, *B* and *C*), consistent with the results obtained by luciferase reporter analysis. In addition, coexpression of FLAG-p73α and FLAG-PKA-Cβ resulted in a slight increase in the amounts of FLAG-p73α, whereas FLAG-PKA-Cβ had a negligible effect on the amounts of FLAG-p73β and FLAG-p53 (Fig. 4). FLAG-p73α decayed at slower rates in the presence of FLAG-PKA-Cβ than in its absence (data not shown); however, its physiological implications remain to be determined.

PKA-Cβ Phosphorylates p73—To determine whether p73 could be a substrate for PKA-Cβ, the GST-p73α fusion proteins used for the *in vitro* pull-down assay were incubated with the commercially available PKA catalytic subunit purified from bovine heart and [γ-^{32}P]ATP. Of the GST-p73α fusion proteins tested, only GST-p73α-(1–130) was phosphorylated by the PKA catalytic subunit (Fig. 5*A*). The N-terminal region of p73α might be involved in phosphorylation by the PKA catalytic subunit.

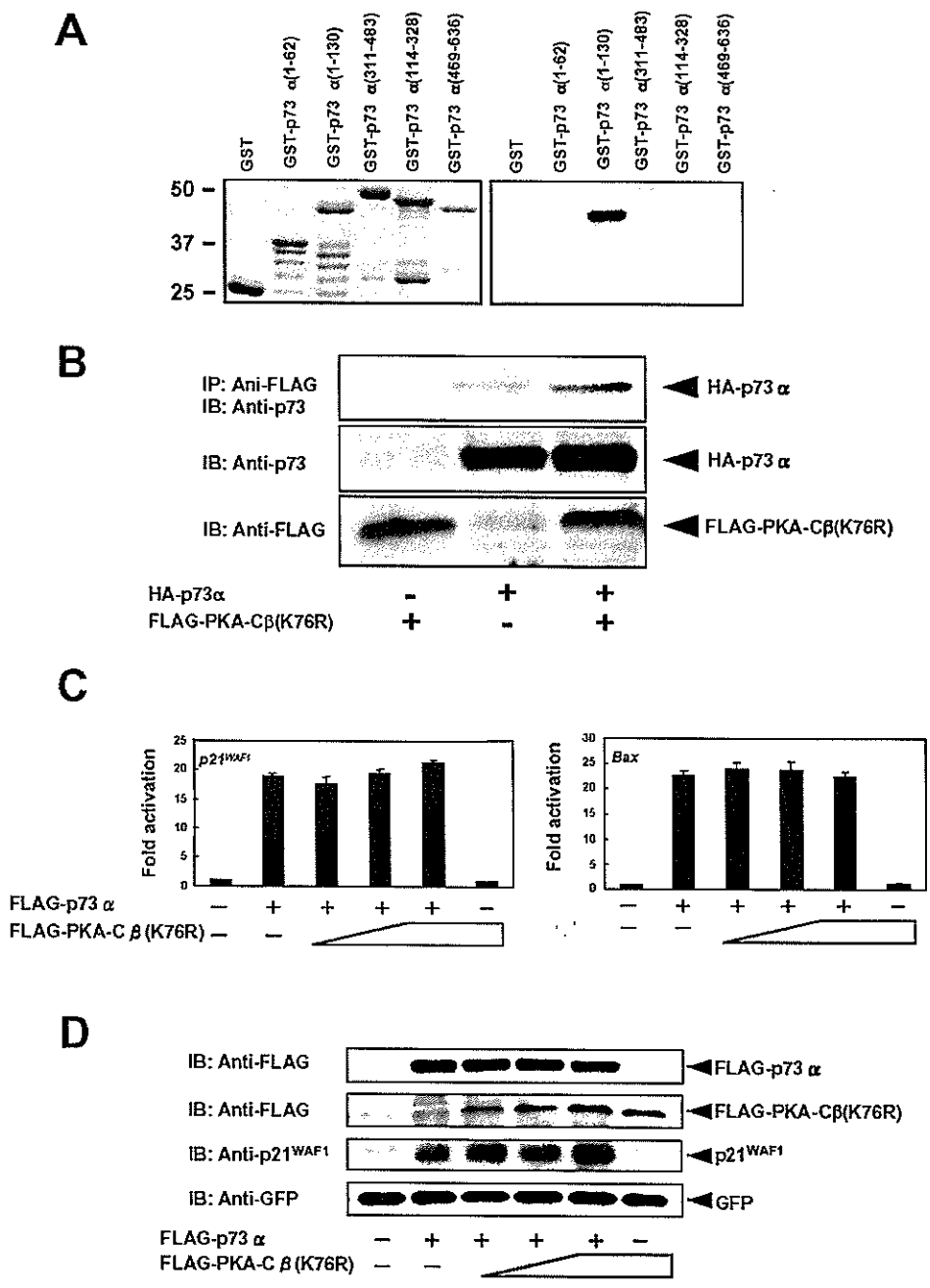

FIG. 5. **PKA-Cβ phosphorylates p73α, and the kinase-deficient mutant of PKA-Cβ fails to inhibit the transcriptional activity of p73α.** *A*, PKA-Cβ can phosphorylate p73α *in vitro*. GST or GST-p73α fusion proteins bound to glutathione-Sepharose beads were incubated with the purified catalytic subunit of PKA in the presence of [γ-^{32}P]ATP for 30 min at 30 °C. Samples were then directly boiled in 2× SDS sample buffer prior to loading them onto 10% SDS-polyacrylamide gels. Following electrophoresis, gels were dried and processed for autoradiography (*right panel*). GST and GST-p73α fusion proteins were stained with Coomassie Brilliant Blue and used for *in vitro* kinase assay (*left panel*). The positions of molecular mass markers are shown on the left in kilodaltons. *B*, kinase-deficient PKA-Cβ retains the ability to interact with p73α. Whole cell lysates prepared from COS-7 cells transiently cotransfected with the indicated combinations of expression plasmids were immunoprecipitated (*IP*) with anti-FLAG monoclonal antibody, and the immunoprecipitates were analyzed by immunoblotting (*IB*) with anti-p73 monoclonal antibody (*upper panel*). Lysates not subjected to immunoprecipitation were analyzed by immunoblotting with anti-p73 (*middle panel*) or anti-FLAG (*lower panel*) monoclonal antibody. *C*, luciferase reporter analysis. H1299 cells were transiently cotransfected with a constant amount of the expression plasmid encoding FLAG-p73α, the luciferase reporter construct carrying the p53/p73-responsive element derived from the p21^{WAF1} (*left panel*) or *bax* (*right panel*) promoter, and pRL-TK in the presence or absence of increasing amounts of the expression plasmid for FLAG-PKA-Cβ(K76R). Forty-eight hours after transfection, luciferase activity was determined as described in the legend to Fig. 4. *D*, PKA-Cβ(K76R) has no detectable effect on the p73α-dependent induction of endogenous p21^{WAF1}. H1299 cells were transiently cotransfected with 200 ng of the expression plasmid for FLAG-p73α and 50 ng of the GFP expression plasmid with or without increasing amounts of the expression plasmid for FLAG-PKA-Cβ(K76R) (200, 400, and 800 ng). Thirty-six hours after transfection, whole cell lysates were prepared and analyzed by immunoblotting for the expression levels of endogenous p21^{WAF1}. The GFP expression plasmid was included as a control for transfection efficiency.

Next, we examined whether the inhibitory effect of PKA-Cβ on the transcriptional activity of p73α is dependent on its kinase activity. As described previously (33, 34), PKA-Cβ(K76R), in which Lys-76 within the ATP-binding motif is replaced with Arg, showed very little catalytic activity. We therefore constructed an expression plasmid for FLAG-PKA-Cβ(K76R) and tested whether PKA-Cβ(K76R) could bind to p73α and also repress p73α-mediated transcriptional activation. Co-immunoprecipitation experiments demonstrated that, like wild-type PKA-Cβ, the kinase-deficient form of PKA-Cβ bound to FLAG-p73α in cells (Fig. 5*B*). Notably, luciferase reporter analysis revealed that FLAG-PKA-Cβ(K76R) had little effect on the ability of p73α to drive transcription from the p21^{WAF1} and *bax* promoters (Fig. 5*C*). In accordance with the results from luciferase reporter analysis, FLAG-PKA-Cβ(K76R) failed to reduce the expression levels of endogenous p21^{WAF1} induced by FLAG-p73α as examined by immunoblotting (Fig. 5*D*). Taken together, these results strongly suggest that PKA-Cβ inhibits p73α-mediated transcriptional activation by a kinase activity-dependent mechanism.

Reduction in the Pro-apoptotic Activity of p73α by PKA-Cβ upon DNA Damage—To extend the functional consequences of the interaction between p73α and PKA-Cβ, we investigated whether PKA-Cβ could affect the pro-apoptotic function of p73α in response to DNA damage. For this purpose, we used a low apoptotic dose of camptothecin to facilitate the detection of a potential induction mediated by p73α. H1299 cells were transiently cotransfected with the expression plasmid for FLAG-p73α or FLAG-p53 with or without the expression plasmid encoding FLAG-PKA-Cβ or FLAG-PKA-Cβ(K76R) and then treated with camptothecin at a final concentration of 1 μM for 24 h. After camptothecin action, cell viability was examined by cell survival assay. As shown in Fig. 6*A*, H1299 cells expressing FLAG-p73α alone exhibited an enhanced sensitivity to apoptosis following exposure to camptothecin, which was consistent with previous observations (35). Of note, coexpression of FLAG-PKA-Cβ and FLAG-p73α resulted in a reduction in the cellular

sensitivity to camptothecin, whereas kinase-deficient PKA-Cβ had no significant effect on cell viability. As was also observed in H1299 cells expressing FLAG-p73α, ectopic expression of FLAG-p53 enhanced camptothecin-induced apoptosis (Fig. 6*B*). In sharp contrast to p73α, wild-type or kinase-deficient PKA-Cβ had a negligible effect on p53.

cAMP Analog Inhibits p73α-mediated Transcriptional Activation—Given the inhibitory effect of exogenous PKA-Cβ on p73α in transfected cells, we sought to determine whether the activation of PKA attenuates p73α-mediated transcriptional activation. H1299 cells were transiently cotransfected with or without the expression plasmid for HA-p73α along with the luciferase reporter construct driven by the p53/p73-responsive element from the $p21^{WAF1}$ or *bax* promoter. Twenty-four hours after transfection, cells were either left untreated or treated with the PKA-activating agent dibutyryl cAMP (Bt_2cAMP) in the presence or absence of the PKA inhibitor H-89. As shown in Fig. 7*A*, Bt_2cAMP treatment inhibited p73α-induced $p21^{WAF1}$ and *bax* promoter activation. Intriguingly, the inhibitory effect of Bt_2cAMP was attenuated when cells were exposed to H-89. Under the identical experimental conditions, endogenous $p21^{WAF1}$ was significantly induced by exogenously expressed HA-p73α (Fig. 7*B*). Densitometric scanning of the immunoblot revealed that Bt_2cAMP treatment decreased the level of $p21^{WAF1}$ by 29% relative to that induced by HA-p73α, and the $p21^{WAF1}$ level was partially restored in the presence of H-89, in accordance with the results obtained by luciferase reporter analysis. Thus, it is likely that the elevation of intracellular cAMP and the subsequent PKA activation contribute to the reduction in p73α-mediated transcriptional activation.

PKA-Cβ Stimulates the Intramolecular Interaction of p73—To clarify the precise molecular mechanism by which PKA-Cβ impairs the transcriptional activity of p73α, we performed ChIP analysis. Cross-linked chromatin prepared from H1299 cells transiently cotransfected with the indicated combinations of expression plasmids was immunoprecipitated with anti-HA antibody, followed by amplification with the indicated promoter-specific primers. Under our experimental conditions, HA-p73α was efficiently recruited to the $p21^{WAF1}$ and *bax* promoters in the absence of exogenous PKA-Cβ (Fig. 8*A*). No significant decrease in chromatin binding was detected in cells expressing HA-p73α and FLAG-PKA-Cβ, suggesting that PKA-Cβ has little effect on the sequence-specific DNA binding activity of p73α.

It has been reported recently that the extreme C-terminal regions of p73α and p63α (another member of the p53 family) have an inhibitory effect on their transactivation potential (7, 36, 37). To assess whether the C-terminal inhibitory domain of p73α could be involved in the PKA-Cβ-mediated down-regulation of p73α, we performed additional luciferase reporter analyses in H1299 cells cotransfected with the expression plasmid for HA-p73α-(1–548) and FLAG-PKA-Cβ. As shown in Fig. 8*B* (*upper panel*), HA-p73α-(1–548), which lacks the extreme C-terminal extension of wild-type p73α, interacted with FLAG-PKA-Cβ as determined by co-immunoprecipitation experiments. It is worth noting that, in contrast to wild-type p73α, FLAG-PKA-Cβ had no detectable effect on the transcriptional activity of HA-p73α-(1–548) (Fig. 8*B*, *lower panel*), indicating that the extreme C-terminal region of p73α plays a critical role in the PKA-Cβ-mediated inhibition of p73α.

Serber *et al.* (37) reported that the extreme C-terminal domain binds to the N-terminal transactivation domain of p63 and inhibits its transactivation potential. Considering that PKA-Cβ interacts with p73α through its N- and C-terminal domains, it is possible that PKA-Cβ could stimulate the intramolecular interaction between the two domains of p73α, thereby inhibiting its transcriptional activity. To test this possibility, we performed co-immunoprecipitation analysis. Whole cell lysates prepared from COS-7 cells transiently transfected with the indicated combinations of expression plasmids were immunoprecipitated with anti-p73 antibody, followed by immunoblotting with anti-HA antibody, and the possible effect of FLAG-PKA-Cβ on the complex formation between HA-p73α-(1–247) and FLAG-p73α-(247–636) was examined. The anti-p73 antibody used for this assay recognizes the C-terminal portion of p73 and thus does not detect p73α-(1–247). As shown in Fig. 8*C*, HA-p73α-(1–247) efficiently co-immunoprecipitated with FLAG-p73α-(247–636) in the presence of FLAG-PKA-Cβ, whereas FLAG-PKA-Cβ(K76R) had a negligible effect on the complex formation between HA-p73α-(1–247) and FLAG-p73α-(247–636). The few complexes observed in the absence of FLAG-PKA-Cβ could be due to endogenous PKA-Cβ. These results strongly suggest that FLAG-PKA-Cβ contributes to the intramolecular interaction of p73α between the N-terminal transactivation and C-terminal inhibitory domains.

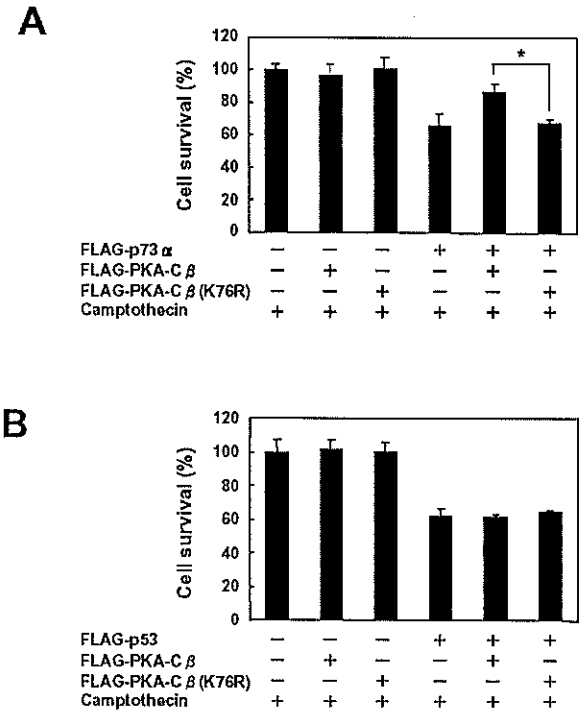

FIG. 6. **p73α-mediated increase in sensitivity to camptothecin is suppressed by wild-type PKA-Cβ, but not by kinase-deficient PKA-Cβ.** H1299 cells were transiently cotransfected with the expression plasmid for FLAG-p73α (*A*) or FLAG-p53 (*B*) with or without the expression plasmid encoding FLAG-PKA-Cβ or FLAG-PKA-Cβ(K76R). Twenty-four hours after transfection, cells were exposed to camptothecin (final concentration of 1 μM) for 24 h, and their viability was evaluated by 3-(4,5-dimethylthiazol-2-yl)-2,5-diphenyltetrazolium bromide assay. *, $p < 0.01$ *versus* +FLAG-PKA-Cβ.

DISCUSSION

In this study, we have screened a human fetal brain cDNA library using a new CytoTrap yeast two-hybrid screening method based on the Sos recruitment system and identified, for the first time, PKA-Cβ as a p73α-binding protein. PKA-Cβ associated with p73α through its N- and C-terminal regions in mammalian cultured cells and significantly inhibited its transactivation function. Under our experimental conditions, PKA-Cβ, which did not bind to p53, had a negligible effect on p53. Intriguingly, PKA-Cβ might bridge the N-terminal transactivation and C-terminal inhibitory domains of p73α, thereby rendering p73α a latent inactive form. *In vitro* kinase assay demonstrated that PKA can phosphorylate p73, and the kinase-deficient mutant of PKA-Cβ (PKA-Cβ(K76R)) failed to

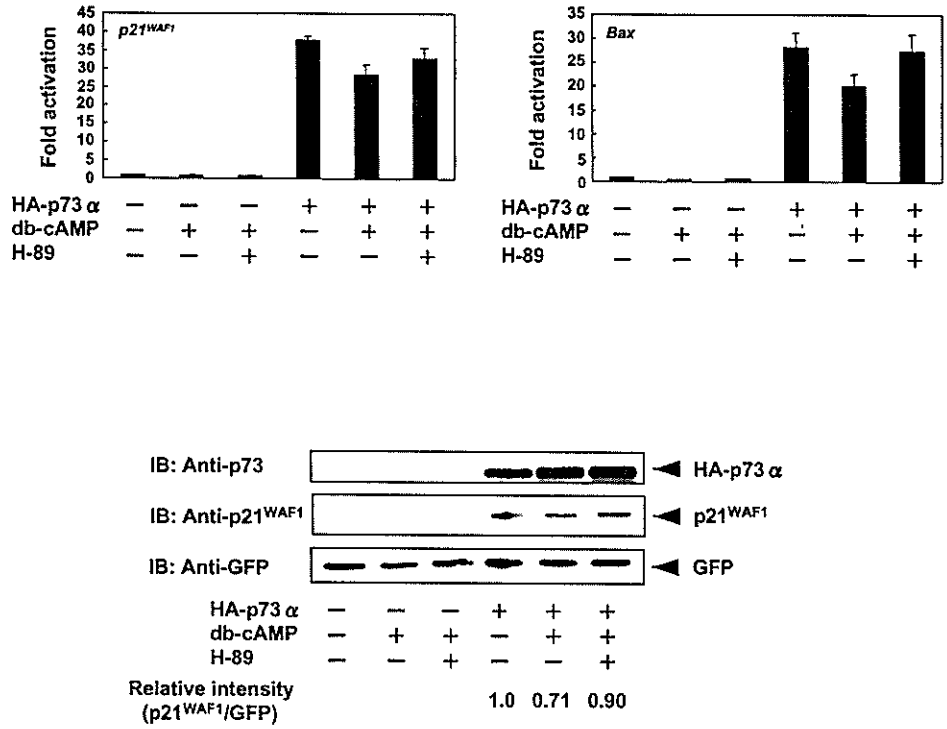

FIG. 7. **Effects of Bt_2cAMP on p73α-mediated transcriptional activation.** *A*, luciferase reporter analysis. H1299 cells were transiently cotransfected with 25 ng of the expression plasmid for HA-p73α, 100 ng of the luciferase reporter construct containing the p53/p73-responsive element derived from the $p21^{WAF1}$ (*left panel*) or *bax* (*right panel*) promoter, and 10 ng of pRL-TK. Twenty-four hours after transfection, cells were left untreated or were treated with Bt_2cAMP (*db-cAMP*; 1 mM) or with Bt_2cAMP (1 mM) plus the PKA inhibitor H-89 (10 μM) for 24 h. Cell lysates were then prepared and subjected to the determination of luciferase activity as described in the legend to Fig. 4. *B*, immunoblot analysis for $p21^{WAF1}$. H1299 cells were transiently cotransfected with 200 ng of the expression plasmid for HA-p73α and 50 ng of the GFP expression plasmid. Twenty-four hours after transfection, cells were treated with or without Bt_2cAMP (1 mM) in the presence or absence of H-89 (10 μM) for 24 h. Whole cell lysates were then prepared and subjected to immunoblotting (*IB*) with the indicated antibodies. Densitometry was used to quantify the amounts of $p21^{WAF1}$, which were normalized to GFP.

reduce the transcriptional activity of p73α, suggesting that the kinase activity of PKA-Cβ is required for its inhibitory effect on p73α. In accordance with these results, the transient activation of the cAMP/PKA signaling pathway by Bt_2cAMP reduced p73α-mediated transcriptional activation, whereas the inhibitory effect of Bt_2cAMP was attenuated when cells were exposed to H-89, a specific pharmacological inhibitor of PKA. Collectively, our present findings indicate that the PKA-mediated phosphorylation and conformational alteration of p73α might be a novel inhibitory mechanism of its activity.

As described previously (38), the PKA catalytic subunit family is composed of three isoforms: PKA-Cα, PKA-Cβ, and PKA-Cγ. PKA-Cα is expressed ubiquitously, whereas PKA-Cβ is expressed predominantly in brain and reproductive tissues (31, 32). PKA-Cβ is expressed as at least six variants (Cβ1, Cβ2, Cβ3, Cβ4, Cβ4ab, and Cβ4abc) arising from alternative splicing of the primary transcript (39). These splice variants contain a unique N terminus, but share a common catalytic domain, suggesting that they have similar enzymatic activity. Sequence analysis revealed that the PKA-Cβ we identified in this study is PKA-Cβ4ab. According to our *in vitro* phosphorylation assay using various truncated forms of GST-p73α as substrates, the N-terminal region of p73α (residues 1–130) might contribute to phosphorylation by PKA. As described previously (40, 41), the amino acid sequence (R/K)*XX*(S/T) is a consensus motif for PKA-dependent phosphorylation. Examination of the amino acid sequence of p73α for a putative PKA recognition site(s) showed three related motifs (^{78}RAAS^{81}, ^{164}KVST^{167}, and ^{402}KLPS^{405}). Ser-81 exists in the N-terminal region of p73α. It is thus likely that this site could be one of the site(s) phosphorylated by PKA, although there is no direct evidence for this possibility. Because PKA-Cβ(K76R), which retained the ability to bind to p73α, failed to inhibit p73α-mediated transcriptional activation, it is conceivable that the PKA-dependent phosphorylation of p73α might serve to modulate its function. Accumulating evidence suggests that, as for p53, post-translational modifications such as phosphorylation and acetylation regulate p73. In response to DNA-damaging agents, p73 is phosphorylated at Tyr-99, Ser-289, and Ser-47 by c-Abl, the protein kinase Cδ catalytic fragment, and Chk1, respectively (16–19, 25). Each of these phosphorylations is associated with the activation of p73. Alternatively, Pin1 recognizes phosphorylated Ser-412, Thr-442, and/or Thr-482 of p73, thereby activating p73 in association with the enhanced levels of its acetylation mediated by p300 (28). On the other hand, cyclin-dependent protein kinase-dependent phosphorylation of p73 at Thr-86 results in a significant reduction of the transcriptional activity of p73 (42). Accordingly, the identification of the precise phosphorylation site(s) of p73α by PKA is necessary to confirm the functional significance of the PKA-mediated phosphorylation of p73α.

We (36) and others (7, 43) reported that p73α exhibits a low level of transactivation ability relative to that of p73β, suggesting that the C-terminal extension of p73α exerts an inhibitory effect on the transcriptional activity of p73. Another p53 family member (p63) also showed similar results (44). Intriguingly, three-dimensional analysis demonstrated that the C-terminal region of p53 exists in close proximity to the central DNA-binding domain (45). In addition, it has been shown that the C

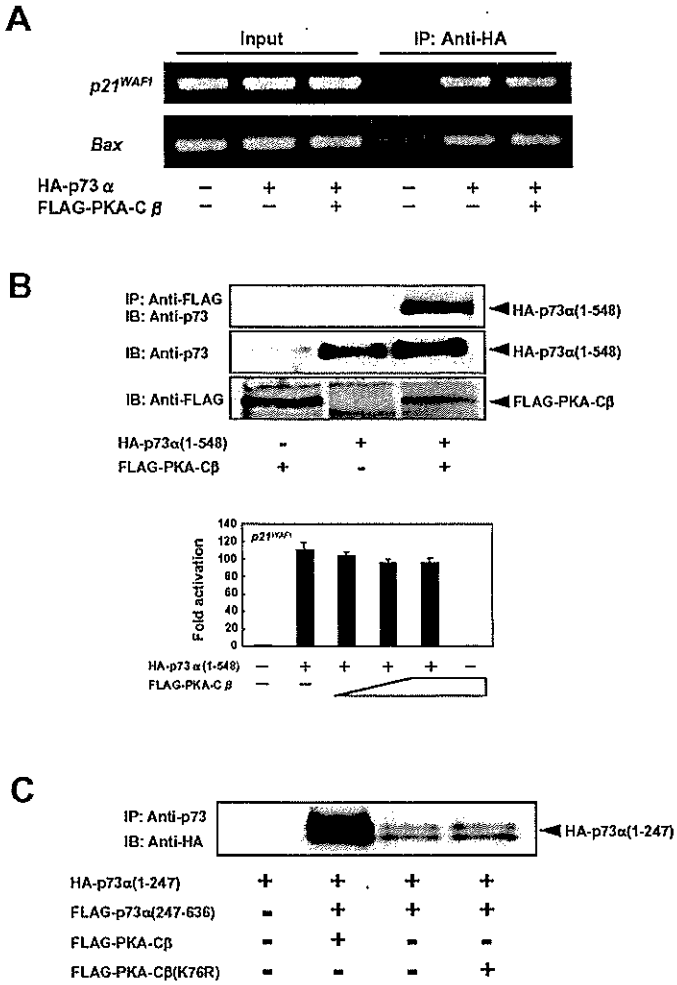

FIG. 8. **PKA-Cβ-mediated intramolecular interaction of p73α contributes to the down-regulation of the transcriptional activity of p73α.** *A*, ChIP assay. H1299 cells were transiently cotransfected with the expression plasmid for HA-p73α or HA-p73α plus FLAG-PKA-Cβ. Thirty-six hours after transfection, cells were fixed in formaldehyde and lysed, and DNA was sheared into 200–500-bp fragments by sonication. HA-p73α-bound DNA was immunoprecipitated (*IP*) with anti-HA monoclonal antibody. The amounts of HA-p73α bound to the p53/p73-responsive element within the $p21^{WAF1}$ (*upper panel*) or *bax* (*lower panel*) promoter region were analyzed by standard PCR. *B*, PKA-Cβ fails to inhibit p73α-(1–548). COS-7 cells were transiently cotransfected with the indicated combinations of expression plasmids. Forty-eight hours after transfection, whole cell lysates were prepared and subjected to co-immunoprecipitation (*first panel*) or immunoblotting (*second* and *third panels*) (*upper panels*). H1299 cells were transiently cotransfected with 25 ng of the expression plasmid for HA-p73α-(1–548), 100 ng of the luciferase reporter construct carrying the p53/p73-responsive element of the $p21^{WAF1}$ promoter, and 10 ng of pRL-TK with or without increasing amounts of the expression plasmid for FLAG-PKA-Cβ (25, 50, and 100 ng). Forty-eight hours after transfection, luciferase activity was determined as described in the legend to Fig. 4 (*lower panel*). *C*, the intramolecular interaction of p73α is stimulated by PKA-Cβ. Whole cell lysates prepared from COS-7 cells transfected with the indicated combinations of expression plasmids were immunoprecipitated with anti-p73 antibody, followed by immunoblotting (*IB*) with anti-HA antibody.

terminus of p53 directly interacts with and masks its DNA-binding domain, thereby inhibiting its DNA binding activity (46, 47). Recently, Serber *et al.* (37) found that the transcriptional activity of p63α is significantly inhibited by an intramolecular interaction. In sharp contrast to p53, the extreme C-terminal region of p63α binds to the N-terminal transactivation domain, but not to the DNA-binding domain, and abrogates its transactivation potential. Given the high amino acid sequence homology between p73α and p63α and their similar domain structure, the transcriptional activity of p73 might be regulated at least in part by an intramolecular inhibitory interaction. According to our *in vitro* pull-down assay, PKA-Cβ bound to the N- and C-terminal regions of p73α. Furthermore, the co-immunoprecipitation experiments demonstrated that p73α-(1–247) efficiently coprecipitated with p73α-(247–636) in the presence of PKA-Cβ, suggesting that PKA-Cβ might promote the intramolecular interaction of p73α to mask the N-terminal transactivation domain rather than the central DNA-binding domain and keep it in an inactive form. Indeed, our ChIP experiments revealed that PKA-Cβ had no significant effect on the DNA binding activity of p73α. Because the kinase-deficient mutant of PKA-Cβ failed to bridge p73α-(1–247) and p73α-(247–636), it is likely that the PKA-mediated phosphorylation of p73 plays an important role in the conformational alteration of p73. However, the precise molecular mechanism by which PKA-mediated phosphorylation could contribute to the inhibition of p73 is currently unknown.

It has been shown previously (48–50) that the activation of PKA has either mitogenic or anti-proliferative effects in mammalian cultured cells and that these opposite responses might be due to the existence of cell type-specific targets of this signaling pathway. Accumulating evidence indicates that the anti-apoptotic effect of PKA might be mediated by the activation of the ERK (extracellular signal-regulated kinase) (51, 52) and phosphatidylinositol 3-kinase/Akt (53, 54) pathways. Recently, Wu *et al.* (55) found that c-Myc enhances the activity of PKA by transactivating the expression of PKA-Cβ. According to their results, constitutive expression of PKA-Cβ results in the promotion of colony formation in soft agar medium, and PKA-Cβ- as well as c-Myc-mediated cellular transformation is markedly inhibited by H-89, suggesting that PKA might be one of the downstream mediators of c-Myc function. As described previously (55–57), PKA directly phosphorylates Bad and glycogen synthase kinase-3β to inhibit their apoptosis-inducing activity. Likewise, our present findings indicate that the PKA-mediated phosphorylation of pro-apoptotic p73 abrogates its function. Thus, it is likely that the anti-apoptotic function of PKA is at least in part due to the inactivation of p73 and the subsequent suppression of apoptotic signaling.

Acknowledgments—We thank members of our laboratory for stimulating discussions and Yuki Nakamura for excellent technical assistance.

REFERENCES

1. Kaghad, M., Bonnet, H., Yang, A., Creancier, L., Biscan, J. C., Valent, A., Minty, A., Chalon, P., Lelias, J. M., Dumont, X., Ferrara, P., McKeon, F., and Caput, D. (1997) *Cell* **90**, 809–819
2. Jost, C. A., Marin, M. C., and Kaelin, W. G., Jr. (1997) *Nature* **389**, 191–194
3. De Laurenzi, V., Costanzo, A., Barcaroli, D., Torrinoni, A., Falcico, M., Annicchiarico-Petruzzelli, M., Levrero, M., and Melino, G. (1998) *J. Exp. Med.* **188**, 1763–1768
4. Di Como, C. J., Gaiddon, C., and Prives, C. (1999) *Mol. Cell. Biol.* **19**, 1438–1449
5. Steegenga, W. T., Shvarts, A., Riteco, N., Bos, J. L., and Jochemsen, A. G. (1999) *Mol. Cell. Biol.* **19**, 3885–3894
6. Zeng, X., Chen, L., Jost, C. A., Maya, R., Keller, D., Wang, X., Kaelin, W. G., Jr., Oren, M., Chen, J., and Lu, H. (1999) *Mol. Cell. Biol.* **19**, 3257–3266
7. Ueda, Y., Hijikata, M., Takagi, S., Chiba, T., and Shimotohno, K. (1999) *Oncogene* **18**, 4993–4998
8. De Laurenzi, V., Catanl, M. V., Teminoni, A., Corazzari, M., Melino, G., Costanzo, A., Levrero, M., and Knight, R. A. (1999) *Cell Death Differ.* **6**, 389–390
9. Ishimoto, O., Kawahara, C., Enjo, K., Obinata, M., Nukiwa, T., and Ikawa, S. (2002) *Cancer Res.* **62**, 636–641
10. Yang, A., Walker, N., Bronson, R., Kaghad, M., Oosterwegel, M., Bonnin, J., Vagner, C., Bonnet, H., Dikkens, P., Sharpe, A., McKeon, F., and Caput, D. (2000) *Nature* **404**, 99–103
11. Pozniak, C. D., Radinovic, S., Yang, A., McKeon, F., Kaplan, D. R., and Miller, F. D. (2000) *Science* **289**, 304–306
12. Stiewe, T., Zimmermann, S., Frilling, A., Esche, H., and Putzer, B. M. (2002) *Cancer Res.* **62**, 3598–3602
13. Grob, T. J., Novak, U., Maisse, C., Barcaroli, D., Luthi, A. U., Pirnia, F., Hugli, B., Graber, H. U., De Laurenzi, V., Fey, M. F., Melino, G., and Tobler, A. (2001) *Cell Death Differ.* **8**, 1213–1223
14. Nakagawa, T., Takahashi, M., Ozaki, T., Watanabe, K., Todo, S., Mizuguchi, H., Hayakawa, T., and Nakagawara, A. (2002) *Mol. Cell. Biol.* **22**, 2575–2585

15. Zaika, A. I., Slade, N., Erster, S. H., Sansome, C., Joseph, T. W., Pearl, M., Chalas, E., and Moll, U. M. (2002) *J. Exp. Med.* **196,** 765–780
16. Gong, J., Costanzo, A., Yang, H. Q., Melino, G., Kaelin, W. G., Jr., Levrero, M., and Wang, J. Y. (1999) *Nature* **399,** 806–809
17. Agami, R., Blandino, G., Oren, M., and Shaul, Y. (1999) *Nature* **399,** 809–813
18. Yuan, Z.-M., Shioya, H., Ishiko, T., Sun, X., Gu, J., Huang, Y. Y., Lu, H., Kharbanda, S., Weichselbaum, R., and Kufe, D. (1999) *Nature* **399,** 814–817
19. Ren, J., Datta, R., Shioya, H., Li, Y., Oki, E., Biedermann, V., Bharti, A., and Kufe, D. (2002) *J. Biol. Chem.* **277,** 33758–33765
20. Yuan, Z.-M., Utsugisawa, T., Ishiko, T., Nakada, S., Huang, Y., Kharbanda, S., Weichselbaum, R., and Kufe, D. (1998) *Oncogene* **16,** 1643–1648
21. Sun, X., Wu, F., Datta, R., Kharbanda, S., and Kufe, D. (2000) *J. Biol. Chem.* **275,** 7470–7473
22. Sanchez, Y., Wong, S., Thoma, R. S., Richman, R., Wu, Z., Piwnica-Worms, H., and Elledge, S. J. (1997) *Science* **277,** 1497–1501
23. Liu, Q., Guntuku, S., Cui, X. S., Matsuoka, S., Cortez, D., Tamai, K., Luo, G., Carattini-Rivera, S., DeMaya, F., Bradley, A., Donehower, L. A., and Elledge, S. J. (2000) *Genes Dev.* **14,** 1448–1459
24. Zhao, H., and Piwnica-Worms, H. (2001) *Mol. Cell. Biol.* **21,** 4129–4139
25. Gonzalez, S., Prives, C., and Cordon-Cardo, C. (2003) *Mol. Cell. Biol.* **23,** 8161–8171
26. Zeng, X., Li, X., Miller, A., Yuan, Z., Yuan, W., Kwok, R. P., Goodman, R., and Lu, H. (2000) *Mol. Cell. Biol.* **20,** 1299–1310
27. Costanzo, A., Melro, P., Pediconi, N., Fulco, M., Sartorelli, V., Cole, P. A., Fontemaggi, G., Fanciulli, M., Schiltz, L., Blandino, G., Balsano, C., and Levrero, M. (2002) *Mol. Cell* **9,** 175–186
28. Mantovani, F., Piazza, S., Gostissa, M., Strano, S., Zacchi, P., Mantovani, R., Blandino, G., and Del Sal, G. (2004) *Mol. Cell* **14,** 625–636
29. Watanabe, K., Ozaki, T., Nakagawa, T., Miyazaki, K., Takahashi, M., Hosoda, M., Hayashi, S., Todo, S., and Nakagawara, A. (2002) *J. Biol. Chem.* **277,** 15113–15123
30. Nakamura, Y., Ozaki, T., Nakagawara, A., and Sakiyama, S. (1997) *Eur. J. Cancer* **33,** 1986–1990
31. Uhler, M. D., Chrivia, J. C., and McKnight, G. S. (1986) *J. Biol. Chem.* **261,** 15360–15463
32. Cadd, G., and McKnight, G. S. (1989) *Neuron* **3,** 71–79
33. Taylor, S. S., Buechler, J. A., and Yenemoto, W. (1990) *Annu. Rev. Biochem.* **59,** 971–1005
34. Scott, J. D. (1991) *Pharmacol. Ther.* **50,** 123–145
35. Irwin, M. S., Kondo, K., Marin, M. C., Cheng, L. S., Hahn, W. C., and Kaelin, W. G., Jr. (2003) *Cancer Cells* **3,** 403–410
36. Ozaki, T., Naka, M., Takada, N., Tada, M., Sakiyama, S., and Nakagawara, A. (1999) *Cancer Res.* **59,** 5902–5907
37. Serber, Z., Lai, H. C., Yang, A., Ou, H. D., Sigal, M. S., Kelly, A. E., Darimont, B. D., Duijf, P. H. G., van Bokhoven, H., McKeon, F., and Dotsch, V. (2002) *Mol. Cell. Biol.* **22,** 8601–8611
38. Skalhegg, B. S., and Tasken, K. (2000) *Front. Biosci.* **5,** 678–693
39. Ørstavik, S., Reinton, N., Frengen, E., Langeland, B. T., Jahnsen, T., and Skalhegg, B. S. (2001) *Eur. J. Biochem.* **268,** 5066–5073
40. Kemp, B. E., Graves, D. J., Benjamin, E., and Krebs, E. G. (1977) *J. Biol. Chem.* **252,** 4888–4894
41. Higuchi, H., Yamashita, T., Yoshikawa, H., and Tohyama, M. (2003) *EMBO J.* **22,** 1790–1800
42. Gaiddon, C., Lokshin, M., Gross, I., Levasseur, D., Taya, Y., Loeffler, J.-P., and Prives, C. (2003) *J. Biol. Chem.* **278,** 27421–27431
43. Lee, C.-W., and La Thangue, N. B. (1999) *Oncogene* **18,** 4171–4181
44. Yang, A., and McKeon, F. (2000) *Nat. Rev. Mol. Cell. Biol.* **1,** 199–207
45. Friend, S. (1994) *Science* **265,** 334–335
46. Hupp, T. R., and Lane, D. P. (1994) *Cold Spring Harbor Symp. Quant. Biol.* **59,** 195–206
47. Hupp, T. R., Sparks, A., and Lane, D. P. (1995) *Cell* **83,** 237–245
48. Smets, L. A., and Van Rooy, H. (1987) *J. Cell. Physiol.* **133,** 395–399
49. Zachary, I., Masters, S. B., and Bourne, H. R. (1990) *Biochem. Biophys. Res. Commun.* **168,** 1184–1193
50. Chen, J., and Iyengar, R. (1994) *Science* **263,** 1278–1281
51. Xia, Z., Dickens, M., Raingeaud, J., Davis, R. J., and Greenberg, M. E. (1995) *Science* **270,** 1326–1331
52. Anderson, C. N., and Tolkovsky, A. M. (1999) *J. Neurosci.* **19,** 664–673
53. Sable, C. L., Filippa, N., Hemmings, B., and Van Obberghen, E. (1997) *FEBS Lett.* **409,** 253–257
54. Filippa, M., Sable, C. L., Filloux, C., Hemmings, B., and Van Obberghen, E. (1999) *Mol. Cell. Biol.* **19,** 4989–5000
55. Wu, K.-J., Mattioli, M. M., Morse, H. C., III, and Dalla-Favera, R. (2002) *Oncogene* **21,** 7872–7882
56. Harada, H., Becknell, B., Wilm, M., Mann, M., Huang, L. J.-S., Taylor, S. S., Scott, J. D., and Korsmeyer, S .J. (1999) *Mol. Cell* **3,** 413–422
57. Li, M., Wang, X., Meintzer, M. K., Laessig, T., Birnbaum, M. J., and Heidenreich, K. A. (2000) *Mol. Cell. Biol.* **20,** 9356–9363